Università
Ca'Foscari
Venezia

Dottorato di ricerca
in Scienze e Tecnologie
Scuola di dottorato in Scienze Ambientali
Ciclo XXIV
(A.A. 2010 - 2011)

Identification and characterization of Fluorescent Protein from marine organisms and potentially applications

SETTORE SCIENTIFICO DISCIPLINARE DI AFFERENZA: BIO/13
Tesi di dottorato di Tiziana Masullo, matricola 955664

Coordinatore del Dottorato

Prof. Bruno Pavoni

Tutori del dottorando

Prof. Marcantonio Bragadin

Dott.ssa Angela Cuttitta

Index

Abstract

Green Fluorescent Protein (GFP) from the hydromedusa *Aequorea victoria* is intensively used in biomedical sciences (Tsien, 1998).

In nature, GFP is a component of the *A. victoria* bioluminescent system. Like many other marine organisms, this jellyfish can produce bright flashes in response to external stimulation. GFP is a secondary emitter that transforms blue light (460 nm), emitted by the Ca^{2+}- dependent photoprotein aequorin, into green light (508 nm) (Johnson *et al*., 1962). Although GFPs similar to *Aequorea* GFP are found in other bioluminescent coelenterates (Chalfie, 1995), the biological significance of blue light transformation is not clear, particularly since the majority of bioluminescent animals do not possess this mechanism. The discovery of GFP-like proteins in the non-bioluminescent Anthozoa species indicates these proteins are not necessarily linked to bioluminescence (Matz *et al*., 1999). In fact, these organisms can produce bright flashes through GFP, as an electromagnetic radiation source with specific wavelength in response to external stimulation (Gurskaya *et al*., 2003).

GFP has a photo protective function (Wiedenmann *et al*., 2000).

Thanks to its peculiar characteristics GFP can be used as a tool to introduce a fluorescent tag into biological system and for example to image when and where a specific protein is being expressed. In fact, Fluorescent Proteins (FPs) are widely used as noninvasive probes to study different biological models from individual cells to whole organisms. The use of FPs enable the tracking of every step of the protein of interest: expression, localization, movement, interaction and activity in the cell, tissue or organism. The main applications of FPs are: visualization of target-gene promoter up- and down-regulation, protein labeling, detection of protein–protein interactions, tracking protein movement and monitoring cellular parameters using FP-based fluorescent sensors.

In recent studies FPs were used to understand the effects of heavy and essential metals on the fluorescence intensity of these proteins (Richmond *et al*., 2000; Bozkurt *and* Cavas, 2008; Chapleau *et al*., 2008; Isarankura *et al*., 2009; Sumner *et al*., 2006; Eli *and* Chakrabartty, 2006; Tansila *et al*., 2008; Rahimi *et al*., 2008).

In this study, two green fluorescent proteins from two distinct species of Cnidaria: *Aequorea coerulescens* (Hydrozoa) and *Anemonia sulcata* (Anthozoa), have been

characterized according to the UV – Visible spectroscopy investigations (absorption and emission). *A. sulcata* was selected for the presence of GFP in the tentacles and for its widely distribution in the Mediterranean sea. So, there was not problem in the sampling of species.

The study of the fluorescence proteins behavior in presence of potentially toxic metal ions was analyzed too. They are stored in the lipid of biological organisms through biomagnifications and bioaccumulations effects when these metals are sedimented in oceans and in earth. Metals are dangerous because when absorbed and metabolized by organisms, they are converted in organic metal composts that, for their structure, are transferred in the cells and interfere with their normal biological functions. This research project had a multi disciplinary approach and it was shown by the different biochemical and biophysical techniques that we adopted to arrive at the goals.

In a preliminary phase of the study, it was necessary to focus the attention on the characterization of pure GFP to acquire the UV – Visible spectroscopy techniques and to choose the best possible condition of assays (buffer solution, concentration, pH, temperature). For this reason the first experiments were conducted on the recombinant GFP of *A. coerulescens* "rAcGFP" (Clontech). It was selected among the others proteins because it derived from a cnidarian species as *A. sulcata* but it was a recombinant and a pure protein. This was considered the control system to compare results obtained on the GFP that was extracted from *A. sulcata* and was partially purified according to the gel filtration.

So, the absorption spectrum of rAcGFP was studied to value the best ratio of signal – noise because the assay conditions allow to use only small protein concentrations. In the second step, the emission spectrum was studied in order to value the shape of fluorescent band, the position of maximum peak and the intensity of fluorescence emission with the change of excitation wavelength. Then, the same spectroscopic measures were conducted in presence of environmental contaminants as cadmium, nickel, lead and copper potentially dangerous for human health. Nickel, cadmium, lead and copper were chose because they had a few oxidation states and did not required specific clean rooms.

Although the greatest sensibility of emission rather the absorption was recorded (at the same protein concentration) the last one was used as control system for the eventually sample precipitation when increasing concentration of metals were added.

For the rAcGFP a small quenching effects (decrease of fluorescence intensity emission) in the emission spectrum were observed. Results, in the observed conditions suggested that the fluorophore had a low capacity to discriminate the presence of different metals solutions. In fact, the metal – protein bond did not seem to be selective and the bond effect unchanged with the different metals investigated.
Then, the interest was focused on *A. sulcata*. In the first step the localization of the GFP according to the confocal microscopy was studied. The presence of fluorescence was observed only in the tentacles portion, in particular the green and the red fluorescence were distributed in two different regions of the tentacles: the green fluorescence in the ectoderm and the red in the gastroderm portion. So, in these portions, the emission spectra were identified as the characteristic spectrum of the GFP of *A. sulcata* and the chlorophyll.

In the second step, the biochemical characterization of total protein extract from the tentacles was conducted (determination of size of fluorescent band and the total protein patterns). Then, the partially purified protein solution (PPS) was obtained from total extract according to the gel filtration with a Sephadex G75. The grade of purification was about 80%.

Finally, the spectroscopic characterization of partially purified sample (PPS) was conducted according the UV – Visible spectroscopy protocol previously selected. As previous assays conducted on *A. coerulescences*, the absorption spectrum of PPS was studied to value the best ratio of signal – noise. The absorption band of AsGFP (*A. sulcata* GFP) was isolated from the PPS, but the in these assays conditions the concentration of GFP was very low. In the second step, the emission spectrum of PPS was studied in order to value the shape of fluorescent bands, the position of maxima peaks and the intensity of fluorescence emission with the change of excitation wavelength. The emission bands of AsGFP were isolated from PPS. So, the first one was used to characterized the fluorescence behavior in presence of the same environmental contaminants used on rAcGFP.

Different results was obtained for AsGFP about the trend and the value of quenching effect on the fluorescent emission for all metals used. In fact, the metal – protein bond seemed to be selective. The bond effect changed with the different metals investigated. The order of quenching on the emission protein was Cu(II)>Pb(II)>Cd(II). Moreover, this effect was more obvious at lower metal concentrations. The copper ability to induce

the quenching effect was determined by its dissolved phase. This suggested that the metal – protein bond occurred using the inner coordination sphere of copper.

The metal selectivity, in particular in the triptophan – copper bond, was assured by the correlation between the effect of enhancing of the trp at 350 nm and the quenching of the fluorophore at 500/519 nm, probably determined by the change of protein conformation.

The future study of the possible modification of cellular and sub cellular tentacle ectodermic portion in presence of metal ions, through in vivo assays on *A. sulcata* and the analysis of the fluorescence behavior of recombinant GFP in the same conditions could allow to think at the system as potential device sensor.

1. INTRODUCTION

1.1. Structure of AsGFP and its chromophore

Anthozoa displays a wide array of colors to which fluorescent proteins contribute in a major way (Wiedenmann, 1997, 2000; Matz *et al.*, 1999; Shagin *et al.*, 2004; Dove *et al.*, 2001). Different types of fluorescent proteins were identified from no bioluminescent organisms (Catala, 1959; Kawaguti, 1944, 1966; Schlichter *et al.*, 1986, 1988; Mazel, 1995, 1997; Doubilet, 1997). For example, the green and orange proteins were found in *Anemonia sulcata* that show similar characteristics as GFP from *A. victoria*. Different papers suggest as the tentacles of *Anemonia* exhibit fluorescence and a red pigment in the tips of its tentacles. The expression of GFPs occurred in the ectoderm of the tentacles (Wiedenmann *et al.*, 2000, Leutenegger *et al.*, 2007). Leutenegger *et al.* (2007) determined that AsGFP contributed ~ 5% to the total soluble cellular protein of non-bleached individuals.

Based on the primary structure, the green fluorescent protein of *Anemonia* consists of 228 aa. The crystal structure of GFP showed a cylindrical fold (diameter of 30 Å and a length of 40 Å), in which the structure is comprised of two regular β-barrels and eleven strands. The α-helix forms the scaffold for the fluorophore. So, this compact domain does not allow at diffusible ligands to interact with the fluorophore (Yang *et al.*, 1996; Nienhaus *et al.* 2006; Ormo *et al.*, 1996; Yang *et al.*, 1996b; Morise *et al.*, 1974; Shimomura, 1979).

Nienhaus *et al.* (2006) described the quaternary structure and found that the asymmetric unit of AsGFP contains two identical tetramers related by a no crystallographic symmetry. They are organized as dimers of dimers, so that two types of subunit interfaces can be differentiated; they are known as antiparallel (between subunits A/B and C/D) and perpendicular (between subunits A/C and B/D) interfaces. Both interfaces involve hydrophobic and hydrophilic interactions (fig. 1).

Relatively at tertiary structure, the monomeric subunits within the tetramers are essentially identical. The backbone topology shows the typical 11-stranded b-barrel fold, with the central α-helix interrupted by the chromophore. The AsGFP structure is similar to that of AvGFP. Backbone structural differences between AsGFP and AvGFP

are most pronounced in the region corresponding to amino acids 138–141 (143–146 in AvGFP) and in the loop region formed by amino acids 195–206 (204–216 in AvGFP).

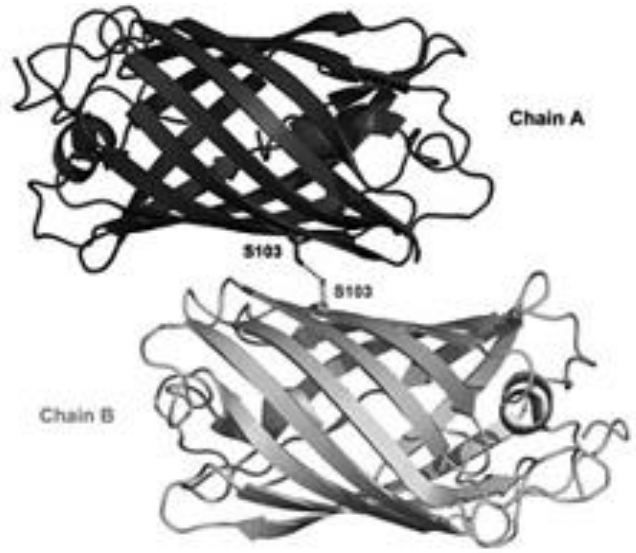

Fig. 1. Interactions network at the AsGFP interfaces. In the A/B interface is evident the interaction of serine 103 with its complement part. (Tasdemir *et al.*, 2008).

The chromophore of AsGFP is a planar resonance system formed autocatalytically by three residues as Gln63, Tyr64, and Gly65 (fig. 2, A and B). The structure is an imidazolinone ring generated by cyclization between the Gln63 and the Gly65 residues and the Tyr64, which is made coplanar with the imidazolinone. Whereas there is a glutamine in the first position of the tripeptide instead of the serine in AvGFP, the AsGFP chromophore is essentially identical to that of AvGFP.

The chromophore of AsGFP is tightly closed within the β-barrel by a hydrogen bonds network. Figure 2 C displays the chromophore cage, with potential hydrogen-bond interactions represented by dashed lines. The highly conserved residues Arg92 and Glu212 have been implicated as being crucially involved in the mechanism of autocatalytic chromophore formation (Ormo *et al.*, 1996; Sniegowski *et al.*, 2005; Wood *et al.*, 2005). The Arg92 guanidinium group hydrogen bonds to the Tyr64-

derived carbonyl oxygen, whereas Glu212 is positioned within hydrogen-bonding distance to the heterocyclic ring nitrogen.

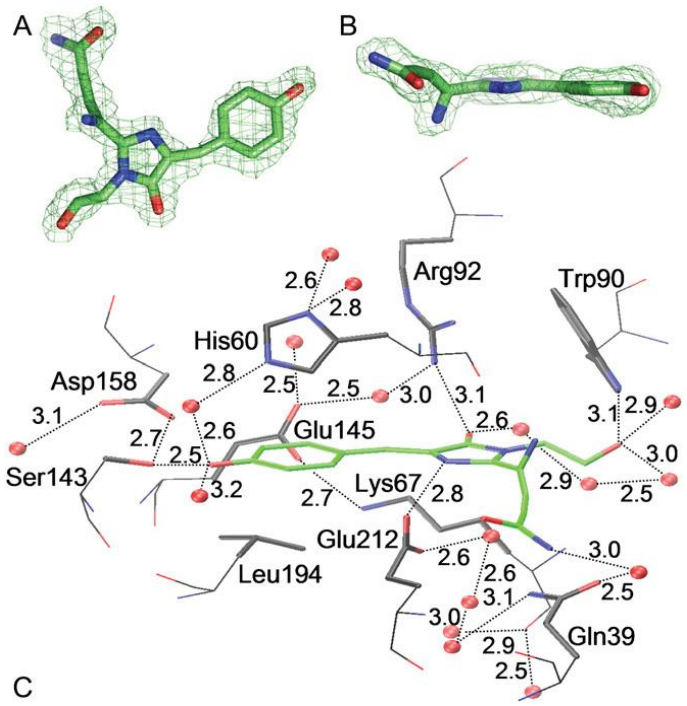

Fig. 2. Electron density map of the AsGFP chromophore (A) Top and (B) side view; (C) Close-up of the AsGFP chromophore (green, carbon; red, oxygen; blue, nitrogen) and surrounding residues (black, carbon; red, oxygen; blue, nitrogen). (Nienhaus *et al.*, 2006)

The resulting structure is a system of conjugated double bonds which is capable of absorbing and emitting light in the visible region.

The Anthozoa GFP-like proteins are known as oligomers (Baird *et al.*, 2000; Mizuno *et al.*, 2001; Wiedenmann *et al.*, 2002; Shagin *et al.*, 2004). This conformation limits their use as fusion tags (Baird *et al.*, 2000; Lauf *et al.*, 2001; Mizuno *et al.*, 2001) but the genetic engineering can solving these problems. For example, Tasdemir and coworkers (2008) modified the tetrameric AsGFP into dimeric and monomeric variants using a particular strategy of sequence alignments.

1.2. Biochemical and Spectral Characteristics of AsGFP

Localization.

Wiedenmann *and* coworkers (2000) defined as the tentacles of *A. sulcata* var. *rufescens* show many pigments under daylight conditions. The ectoderm side (upper) is green, the endoderm (underside) is orange, while the tips have a intense reddish color (fig. 3*A*,*C*). When excited with UV light, the green and the orange pigments emit a bright fluorescence (fig. 3*B*) while the reddish protein is not fluorescent.

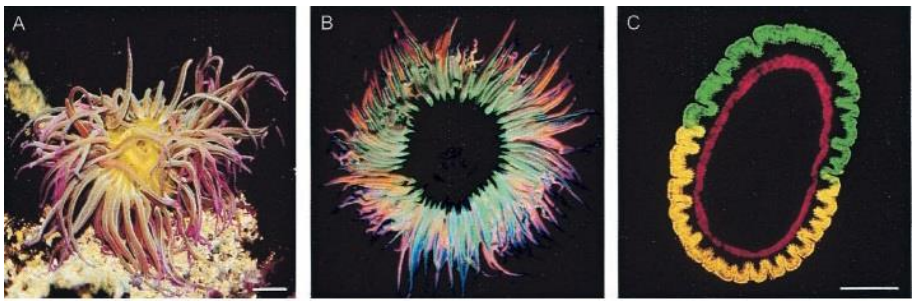

Fig. 3**.** *A. sulcata* var. *rufescens pigments*. (*A*) Pigments exposed under daylight and (*B*) UV (366 nm) conditions. (*C*) Localization of pigments in the kriosection tentacle (20 mm) exposed at UV light. The chlorophyll is shown in red. (Wiedenmann *et al.*, 2000).

Spectral properties.

A solution of partially purified protein showed a green fluorescent emission with two maxima peaks at 499 nm and 522 nm while in the excitation spectrum the peaks were at 480 nm and 511 nm with a shoulder at 400 nm (Table 1 - appendixes) (Wiedenmann *et al.*, 2000). The ratio of the two peaks emission was dependent of the excitation wavelength. In fact, for the authors was evident the existence of two different forms of GFP with $\lambda_{ex\ 480nm}/\lambda_{em499nm}$ and $\lambda_{ex511nm}/\lambda_{em522nm}$. The orange pigment emitted at 595 nm with three maxima excitation peaks at 278 nm, 337 nm, and 574 nm. The red pigment absorbed at 562 nm. Matz *et al.* (1999) distinguished the nomenclature for these proteins of *A. sulcata* var. *rufescens* as: asFP499, asFP522, asFP59 asCP562 (where CP stands for colored protein).

Molecular masses.

Wiedenmann *et al.* (2000) purified these proteins to near homogeneity but AsGFP 499/522 could not be separated through purification assays. This result is indicative of the GFPs occur as oligomers. For the mixed fraction of $AsGFP_{499/522}$ the molecular masses measured 26.2 kDA while for asFP595 and asCP562 was 19.1 kDa. Using gel filtration chromatography the authors compare in physiological and denatured conditions the behavior of these pigments. In the first case all pigments showed a molecular masses of 66 kDa whereas in the second case the oligomers became monomers with a molecular masses of 23 kDa.

Stability.

Fluorescent protein are more stable in different conditions for example high temperature, strong detergent and reducing agent or pH extremes (Table 2. appendixes). asFP595 is more thermo-stable than $AsGFP_{499/522}$ but the last one is more stable when exposed to 1% SDS, 8 M urea, and pH 11. Both proteins are stable when treated with 4% paraformaldehyde (Wiedenmann *et al.*, 2000).

Reversible denaturation.

Wiedenmann *et al.* (2000) studied the behavior of the partially purified extracts of asFP595 and asCP562 in denaturing conditions. After SDS/PAGE and western blot the asFP595 band appeared red if observed under daylight while it emitted orange fluorescence under UV excitation. asCP562 that is a color protein, had the same behavior of renatured asFP595. The renaturation of GFPs is an aspect more studied in literature as results of the restoration of fluorescence (Surpin & Ward, 1989).

The same authors (Wiedenmann *et al.*, 2000) identified the different spectral properties of the two green fluorescent proteins although they could not be separated, so or they had the same molecular weights or represented two states of the same protein.

Using a cDNA library, only in the expressing cells of the sea anemone, seemed to exist a second stable conformation of $AsGFP_{499}$, that was red shifted than the first. Same behavior was found for asFP595 and asCP562 that had the same molecular weight. asCP562 primary structure had all characteristics for the fluorescence emission and its semi-β-can structure could explain this phenomenon. For GFP fluorescence the β-can structure is necessary. For asCP562, the authors (Wiedenmann *et al.*, 2000) proposed

the development of a β-can-like structure in a oligomerization process in which the β-can consists of at least two molecules of color protein. They found for asCP562 and asFP595 an molecular masses of 66 kDa, that corresponded to a tetramer (or four molecules asCP562) (Table 1).

When asFP595 was denatured in absence of β-mercaptoethanol, appeared a second fluorescent band (fig. 4*B*) that migrated at twice the MW of asFP595, then asFP595 consisted of at least two color protein monomers, probably.

The fluorescence emission of $AsGFP_{499}$ had a maximum in a range of pH 6–8 while it decreased at higher pH values (Nienhaus *et al.*, 2006). For pH < 10, the emission peak was at 499 nm with λ_{ex} 480 nm; no other fluorescence emission bands were observed using λ_{ex} 280, 380 and 400 nm, with the exception of the weak tryptophan fluorescence at 340 nm. At pH > 10, a red- shifted (about 18 and 10 nm for absorbance and emission, respectively) observed. At pH < 4 and pH > 12 the protein was unstable.

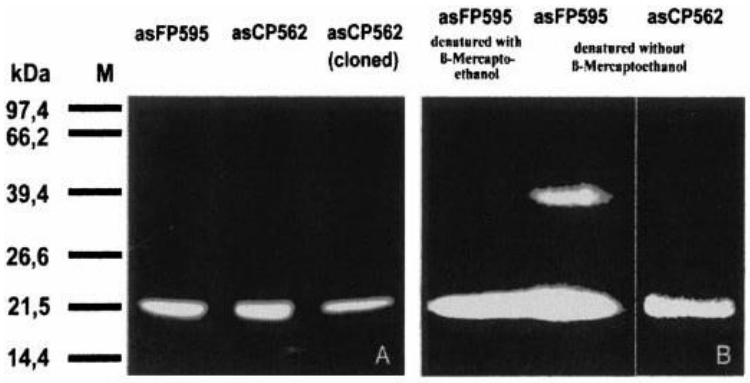

Fig. 4. (*A*) Fluorescence on a nitrocellulose membrane of asFP595, asCP562 and cloned asCP562. (*B*) asFP595 in different denaturation conditions. The second fluorescent band of asFP595 denatured without β-mercaptoethanol is not detectable for asCP562. (Wiedenmann *et al.*, 2000).

In analogy to wild-type AvGFP, the $AsGFP_{499}$ protein showed two bands in the UV/visible spectrum over a wide pH range. Although initially debated (Voityuk *et al.*, 1998), there is now general agreement that the A and B bands are associated with the neutral and anionic states of chromophore (Tsien, 1998). In $AsGFP_{499}$, the two bands were similar in area in the entire pH range in which the protein was stable; and

remarkably, the protonated form of the chromophore became more dominant with increasing pH.

In the structure of $AsGFP_{499}$, amino acid Glu212 is bonded to the chromophore and did not connect to the phenolic oxygen at all. Therefore, proton transfer between the chromophore and Glu212 cannot take place. In addition, the Tyr64 phenol oxygen is connected to the Ser143 hydroxyl by means hydrogen bond, which in turn is hydrogen bonded to Asp158.

The schemes in figure 5, A and B, show the system of two protonatable groups between which protons can be shuttled. The small ratio between neutral and anionic population suggests that only slight differences in free energies occur between the two conformations in the electronic ground state.

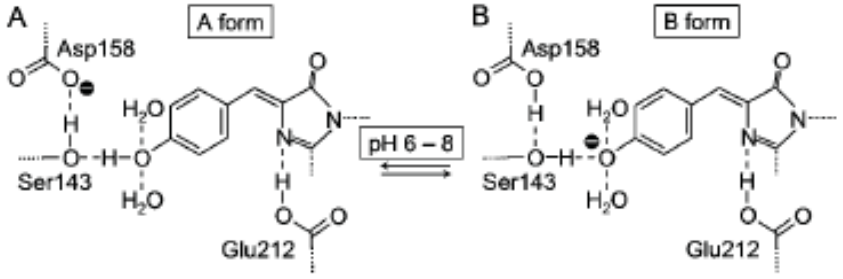

Fig. 5. Representation of the different protonation states of the $AsGFP_{499}$ chromophore and its environment. (Nienhaus *et al*., 2006).

After photon absorption, this balance is disturbed. Phenols become more acidic upon electronic excitation (Tsien, 1998; Voityuk *et al.*, 1998); and then, we suppose efficient excited state proton transfer to Asp158, as is inferred from the observation that excitation in the A and B bands is equally efficient for fluorescence in the 499nm emission band for pH < 8. The Asp158 protonation is a key factor in the proton shuttling mechanism described above.

1.3. Photoswitching of asFP595

Today, a new type of fluorescent proteins have been discovered (Chudakov *et al.*, 2003; Lukyanov *et al.* 2000; Ando *et al*., 2004). These proteins have the characteristic to photoswitch from a fluorescent (on) to nonfluorescent (off) state.

The GFP-like protein asFP595, isolated from the sea anemone *A. sulcata*, is a prototype for such a photoswitchable protein. It is structurally and spectroscopically well characterized (Andresen *et al*., 2005) but its detailed mechanism remains largely unknown.

With the exception of a slight shoulder at 530 nm, the protein displays a single absorption wavelength maximum, which occurs at 572 nm (ε_{572} = 56,200 M^{-1} cm^{-1}) (fig. 6). As is evident asFP595 absorbs efficiently in the middle range of the visible spectrum but remains translucent when excited with blue or long wavelength red light. Consequently, to the observer, the protein appears intensely purple.

asFP595 can be modified by green light from an off state into a on state through blue light irradiation (Lukyanov *et al.*, 2000).

Recently, high-resolution crystal structures of wt asFP595 in its off state (Andresen *et al.*, 2005; Willmann *et al.*, 2005; Quillin *et al.*, 2005), of the Ser158Val mutant in its on state, and of the Ala143Ser mutant in its on and off states (Andresen *et al.*, 2005) were determined (fig 7). The structure of asFP595 chromophore is similar to the others GFPs while the quantum yield is minor than the GFP variants (Ormo *et al.*, 1996; Wall *et al.*, 2000; Yang *et al.*, 1996). The tripeptide is M63-Y64-G65 and the structure is an obligate tetramer with ~ 50% of identity in amino acid sequence as Cnidarian FPs.

In the backbone, the interface between C62 and the chromophore is broken. Andresen and coworkers (2005) defined "*the former M63 Cα and backbone nitrogen atoms are in plane with the imidazolinone ring and, thus, part of the conjugated system. The imino group expands the conjugated system of MYG, likely accounting for the shift of the absorption maximum toward a longer wavelength (572 nm) as compared with that of GFP (470 nm). The MYG chromophore of the off state asFP595 exclusively adopts the trans conformation"*. Spectroscopic data strongly suggested that the photoswitching of asFP595 is accompanied by protonation- state changes of the chromophore (Chudakov *et al.*, 2003).

Andresen *et al.* (2005) indicated that the key factor in asFP595 is a *bottom hula twist* (HTbot) process that is a trans-cis isomerization of the chromophore. The on state is associated to the *cis* conformation (Chudakov *et al.*, 2003).

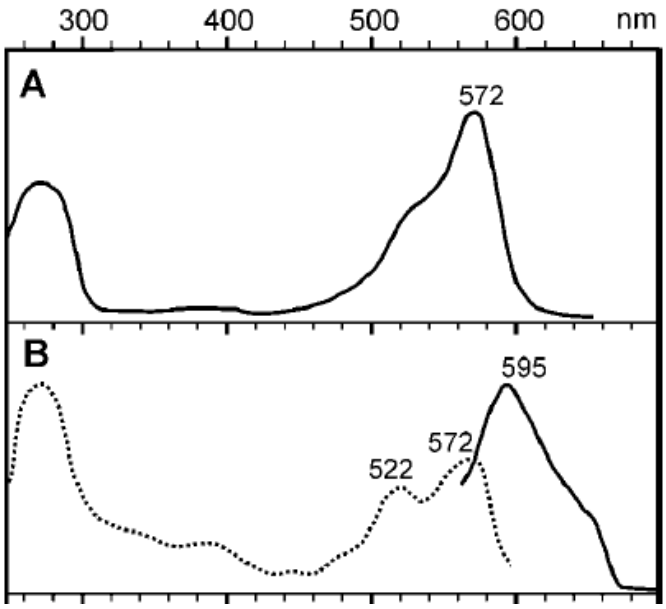

Fig. 6. Spectral characterization of asFP595. *A*, the absorption band of wild-type asFP595. *B*, the excitation (*dotted line*) and emission (*solid line*) band of wt asFP595. (Lukyanov *et al.*, 2000).

The kindling mechanism (Schafer *et al.*, 2007; Andresen *et al.*, 2005) is depicted in figure 8. Before the absorption, the chromophore is in the dark trans state but when the photon arrives it changes in the cis state. The isomerization increases the acidity of the imidazolinone NH proton of the zwitterion and induces the proton transfer to Glu215 (state A-cis, figure 8).

The proton transfer also inhibits the photoisomerization of the zwitterionic species that back to the initial dark trans state. Next, the anionic cis intermediate is protonated at the phenolate oxygen atom to finally yield the stable neutral chromophore (state N-cis).

This situation is similar to that in GFP, where the neutral protonation state is also preferred for the cis chromophore (Helms, 2002; Stoner-Ma *et al.*, 2005; Agmon, 2005; Leiderman *et al.*, 2006; Vendrell *et al.*, 2006). GFP fluorescence originates from the anionic chromophore, which is formed through excited-state proton transfer.

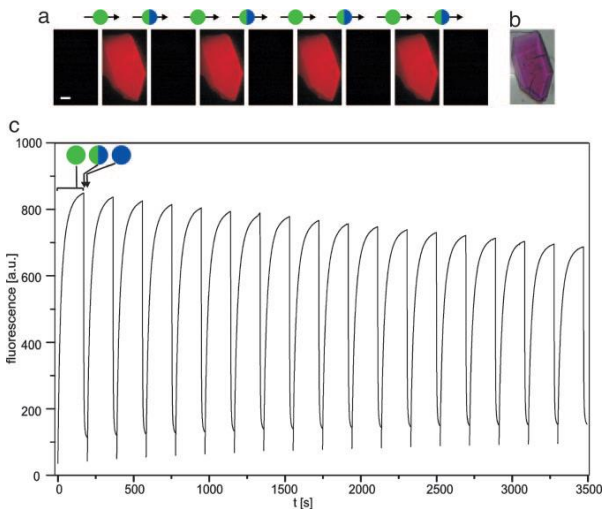

Fig. 7. Photoswitching of (*a*) asFP595-A143S crystals in the equilibrium state. Irradiation with green determine a bright fluorescence that is quenched by irradiation with blue light; (*b*) Image of the crystal protein; (*c*) On/off mechanism of protein fluorescence (Andresen *et al.*, 2005).

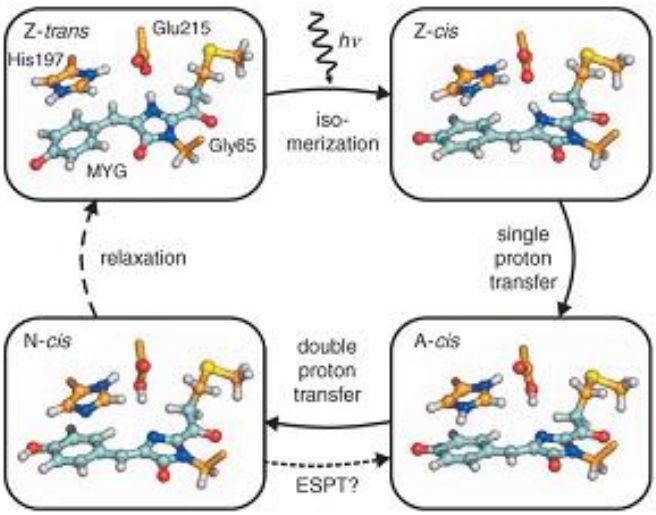

Fig. 8. Kindling mechanism of asFP595.
(Schafer *et al.*, 2007).

1.4. Effects of metals on GFP's fluorescence intensity

Heavy and transition metal ions are distributed widely in biological systems and the environment, and play important roles in many biological and environmental processes (Trautwein, 1997). Excess amount of these ions are, however, toxic. Methods for detecting the presence of one or several of these ions are thus urgently needed, and if the detection method could identify different component of the analytes, it would be an excellent improvement compared with other sensing methods. Although many methods for their analysis have been well developed, existing methods require complex equipments and sophisticated operations. The most widely used techniques for the quantification metals are based on cold vapor atomic absorption spectrometry, anodic stripping voltammetry, X-ray fluorescence spectrometry, neutron activation analysis, inductively coupled plasma mass spectrometry, and atomic fluorescence spectrometry.

Molecular fluorescence is attracting a great deal of interest in environmental monitoring since it is inherently more sensitive than other molecular spectroscopies and so it can be used for the analysis of very low trace concentrations. Recently, the fluorescent proteins from various organisms become potential candidates for sensor development. These include the green fluorescent protein and its variants, the red fluorescent protein (DsRed) from the tropical coral namely *Discosoma sp*.

Richmond *et al*. (2000) have introduced metal-binding sites onto the surface of GFP and found that these metal-binding mutants of GFP exhibited fluorescence quenching at lower transition metal ion (Cu^{2+}, Ni^{2+}, or Co^{2+}) concentrations (10^4) than those of the wild-type protein. This indicated that the mutant proteins were able to bind metal, and that metal ion was close enough to quench the fluorophore, presumable by energy transfer.

Bozkurt *and* Cavas (2008) valued the possible application of the GFP in the development of optical sensors for heavy metal determinations. They analyzed the spectroscopic characteristics of total protein solutions extracted from *A. sulcata* in presence of mercury and found a fluorescence quenching related to green fluorescence protein via Hg(II) (fig. 9). The detection limit was estimated to be 8.2 μg l^{-1} for Hg(II). The order of fluorescence intensities in the existence of other interferent metals was Pb(II) = Sn(II) > Co(II) = Ni(II) > Zn(II) = Cd(II) = Cu(II). No effect of interference they found for Mn(II), Fe(II) and Al(II).

In their study, Chapleau *et al*. (2008) presented a novel fluorescence-based biosensor for the direct monitoring of the uptake and distribution of Hg under noninvasive in vivo conditions. The introduction of a cysteine residue in AvGFP at 205position, converted the protein into a target biosensor for this ion. The binding of metal became more efficient and this was cause of its toxicity. The modified protein showed a decrease of absorbance and fluorescence (fig. 10), that displayed a sigmoidal binding behavior. The detection limit was in the low nano molar range. At very high concentrations of mercury (>200 mM), fluorescence of all tested eGFP variants vanished completely. Treatment with metal-binding agents such as β-mercaptoethanol, glutathione, or EDTA did not regenerated the fluorescence of the protein. These data indicated the high binding of metal to the protein. The crystal structures of mutant protein highlighted the possibility of metal ion access into the protein core. The 205C is located near the hydroxyl group of the tyrosine residues. So, the mutation at this position determines an unusual and irregular conformation and the disruption of the backbone. Many studies suggested as the irregular conformation of the chromophore might determine the solutes introduction into the protein core (Agmon, 2005).

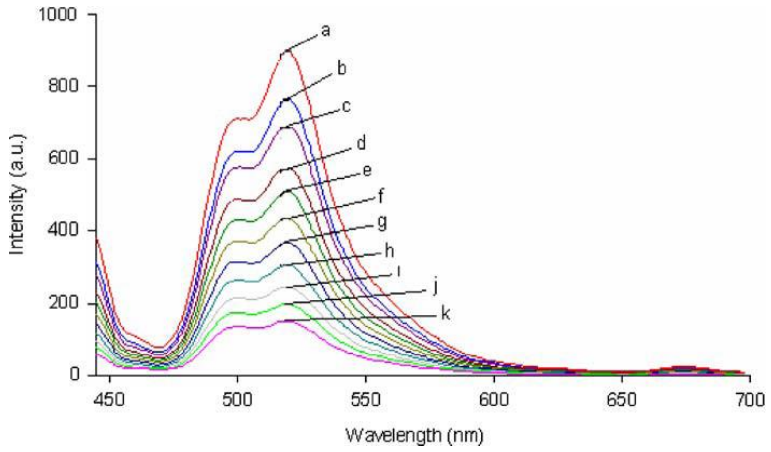

Fig. 9 The quenching emission of GFP supernatants obtained from *Anemonia sulcata var. smaragdina* to various concentrations of Hg(II). (Bozkurt *and* Cavas, 2008).

Isarankura *et al*. (2009) explored spectroscopic determinations of copper ions using chimeric metal-binding green fluorescent protein His6GFP (espressed in *E. coli* and

purified to homogeneity) as an active indicator. Adding copper ions to the GFP, a remarkable decrease of fluorescent intensity was observed. The quenching of fluorescence up to 60% was detected using 500 μM of copper. Different results were obtained with zinc and calcium ions, in which approximately 10–20% of quenching was observed (fig. 11). The addition of EDTA determined the recovery of its original fluorescence. Furthermore, in presence of metal ions, the reduction of the absorbance has been observed. This indicated that the chromophore's ground state was possibly affected by the static quenching process rather than structural or conformational alteration. No significant interference from calcium and magnesium ions was observed on the fluorescent quenching of His6GFP by copper ions.

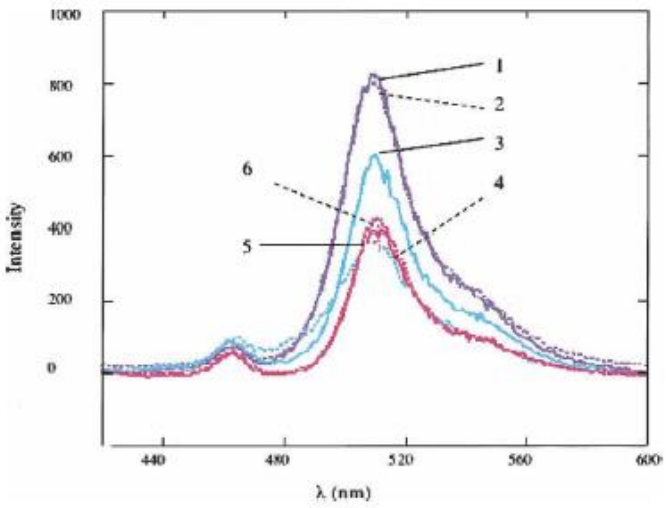

Fig. 10. Emission spectra of eGFP, 203C and 205C in presence of mercury ions (20 mM). 1:eGFP; 2: eGFP + 200mM $HgCl_2$; 3: eGFP205C; 4: eGFP205C + 200 mM $HgCl_2$; 5: eGFP203C; 6: eGFP203 C + 200 mM $HgCl_2$. (Chapleau *et al*., 2008).

Sumner *et al*. (2006) described the quenching effect of Cu^{+} and Cu^{2+} on the fluorescence emission of DsRed (Fradkov *et al*., 2002). They measured a detection limit below 1 ppb. The *wt* DsRed was more sensitive than the engineered and *wt* GFPs. Moreover, they valued if metals as Mn^{2+}, $Fe^{2+/3+}$, Co^{2+}, Ni^{2+}, Zn^{2+}, Cd^{2+}, Ag^{+}, Hg^{2+}, Pb^{2+}, Mg^{2+} or Ca^{2+} competed for the copper binding site, but they did not find interference. Furthermore, they indicated that the quenching was not a collisional type. With EDTA the fluorescence restored at its initial value. It is known that copper ions have affinity

with amines, nitrogens and thiolates (Silvia *and* Williams, 1991); and usually structural motifs are composed of His, Tyr, Glu, Asp, Cys, and sometimes Asn and Gln (Sigel *and* Martin, 1982).

Eli *and* Chakrabartty (2006) investigated on the fluorescence quenching of drFP583 (DsRed) protein and its variants by many metals (Na^{+}, K+, Mg^{2+}, Ca^{2+}, Cr^{2+}, Mn^{2+}, Fe^{2+}, Co^{2+}, Ni^{2+}, Cu^{2+}, and Zn^{2+}). No effects from Na^{+}, K+, Mg^{2+} and Ca^{2+} were observed. The greatest percentage quenching occurred with Cu^{2+} for drFP583 and its mutans while EGFP showed modest quenching (fig. 12). The percentage quenching of the red fluorescence and the green fluorescence was different, 66% versus 22%, respectively.

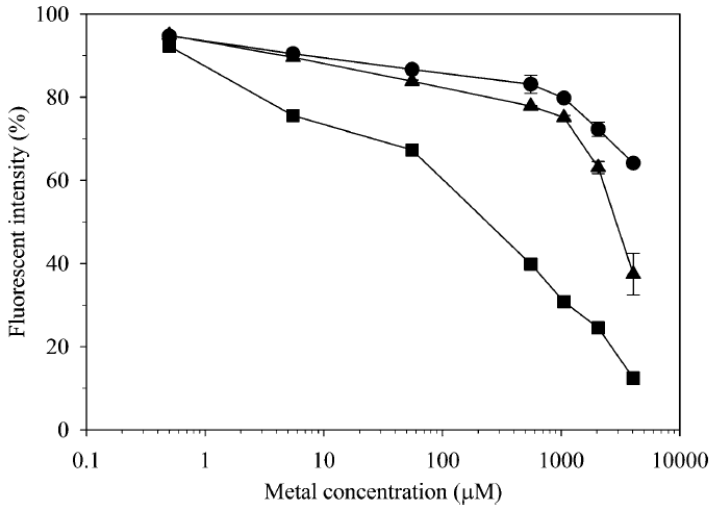

Fig. 11. Dose–response curves of His6GFP against calcium ions (filled circle), zinc ions (filled triangle), or copper ions (filled square). (Isarankura *et al*., 2009).

Tansila *et al*. (2008) valued the metal binding potential of GFP in which they introduced a superfolder mutation and additional mutagenesis for histidines at different position. Each variant responded differently upon interaction with metal ions (Cu^{2+}, Co^{2+}, Mn^{2+}, Ni^{2+} and Zn^{2+}). Cu^{2+} was the only metal which was able to efficiently decrease the fluorescent activity of all proteins, whereas there were no significant effects from Co^{2+}, Mn^{2+} and Ni^{2+}. This was in good agreement with previous studies on copper binding to DsRed, a red fluorescent protein (Sumner *et al*., 2006; Eli *and* Chakrabartty, 2006). The

most sensitive species to copper quenching was the variant with His165. Moreover this variant was enhanced in the presence of Zn^{2+} or Mn^{2+} ions. These data indicated that the locations of introduced histidines are important in the interaction with metal ions. Authors suggested that the enhanced effect was caused by a native histidine at position 148 which can cooperatively function as a metal binding partner to increase the metal sensitivity.

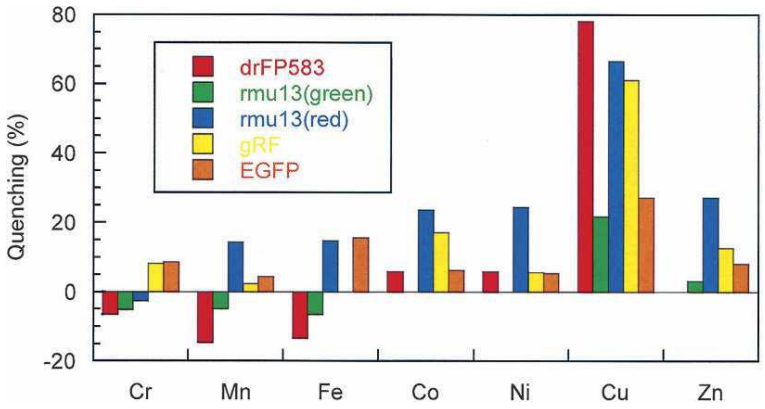

Fig. 12. Quenching of many fluorescent proteins in presence of different metal ions. (Eli *and* Chakrabartty, 2006).

Rahimi *et al*. (2008) have performed spectroscopic investigations to determine the mechanism of quenching of DsRed mutants fluorescence in the presence of Cu^{2+}. Stern-Volmer constants and quenching rate constants supported the observation of static quenching in DsRed in the presence of Cu^{2+}. Circular dichroism (CD)-spectroscopic studies revealed no effect of Cu^{2+}-binding on the secondary structure or conformation of the protein. The effect of pH changes on the quenching of DsRed fluorescence in the presence of copper resulted in pKa values indicative of histidine and cysteine residue involvement in Cu^{2+} binding.

Several metal-specific bacterial sensors with GFP as reporter gene for the detection of metals have been developed. Roberto *et al*. (2002) created a whole cell arsenic biosensor utilizing a GFP reporter gene. Taylor *et al*. (2004) developed a whole-cell fluorescence-based biosensor for nitrate, in which they have optimized the bioassay

conditions so that the fluorescence intensity was proportional to the extracellular nitrate concentration.

Engineered GFPs have been applied for real-time monitoring of intracellular mobility of zinc ions (Isarankura-Na-Ayudhya *et al*., 2005). Low concentration of zinc ions (50 nM) did not determine significant effects on the fluorescent intensity while at higher concentrations (50 μM – 50 mM) the enhanced of signal was observed. Hsiu-Chuan Liao *et al*. (2006) demonstrated that GFP-based bacterial biosensor was useful and applicable in determining the bioavailability of heavy metals with high sensitivity in contaminated sediment and soil samples and suggested a potential for its inexpensive application in environmentally relevant sample tests.

Mizuno *et al*. (2007) created a metal-ion-responsive GFP by the combination of the circularly permutated GFP with the de novo designed metal-ion-binding, trimeric coiled-coil protein. The fluorescence emission was also detected when the combination protein was expressed in *E. coli*, indicating that the protein worked in vivo. Thus, the protein was useful to monitor transition metal ions.

Chakraborty *et al*. (2008) reported GFP expressing bacterial biosensor to measure lead contamination in aquatic environment.

In the study of 2008, Fu *et* al. observed the proximity of single GFPs to metallic silver nanoparticles increases its fluorescence intensity approximately 6-fold and decreases the decay time. Single protein molecules on the silvered surfaces emitted 10-fold more photons as compared to glass prior to photobleaching. The photostability of single GFP has increased to some extent. Accordingly, we observed longer duration time and suppressed blinking. The detection of metal-surface enhanced fluorescence from GFP suggests the more extensive use of metallic nanostructures in imaging and single molecule detection.

2. Spectroscopic characterization of recombinant Green Fluorescent Protein from *Aequorea coerulescens* (rAcGFP) and its behavior in presence of potentially toxic metal ions

2.1. Biology of *Aequorea coerulescens*

A. coerulescens (Brandt, 1838) belongs at Cnidaria phylum, subphylum Medusozoa, superclass Hydrozoa, class Hydroidomedusae. It has about 100 radial canals and about 3-6 times as many tentacles that are bulb laterally compressed. Umbrella up to 145 mm wide is usually 60-80 mm.

The low and thick manubrium is about half as wide as umbrella. The gonads extend along almost whole length of radial canals. It has numerous small bulbs with excretory papillae and statocysts numerous, crowded. It belongs at the zooplankton of the North Pacific Ocean. Although *A. coerulecens* and *A. victoria* look similar, some of their features are clearly different. The most obvious difference is that *A. victoria* carries only 1 tentacle in the radial channel, whereas *A. coerulescens* possesses 3–6 tentacles between each pair of adjacent radial channels.

In contrast to *A. victoria*, *A. coerulescens* medusae displayed blue, not green, luminescence. Gurskaya *et al*. (2003) described for the wild type acGFP no detectable fluorescence under either UV light or using a fluorescence microscope. However, using monoclonal antibodies against GFP they found that a protein extract from *A. coerulescens* contained a GFP-like protein that had the 92% identity at the amino acid level with AvGFP. It was detected in the umbrella border.

All known key GFP residues are conserved in AcGFP, including the chromophore forming Ser65, Tyr66 and Gly67 residues, the evolutionarily invariant Arg96 and Glu222, and His148, Phe165, Ile167 and Thr203 which are all spatially close to the chromophore.

Gurskaya *et al*. (2003) used a random mutagenesis to generate fluorescent mutants of wt GFP of this species. The substituting E222G appeared to be the key event in creating a fluorescent form. Moreover five amino-acid substitutions compared with the wild-type, specifically V11I, F64L, K101E, T206A and E222G determined a very bright mutant.

A pure, stable and monomeric protein (27KDa) rAcGFP (Clontech) was used for the spectroscopic assays.

It was dissolved in MES 20mM at pH 7.2 solution and final concentration of 0.7 µM. This protocol of sample preparation was used in all experiments.

A UV-Vis recording spectrophotometer (Shimadzu) with a 1cm path length cuvette was used for absorbance spectra measurements in a range from 190nm to 900nm (scan speed: medium; sampling interval: 0.5).

The correct concentration of protein was determined using Beer-Lambert law. The molar coefficient extinction ($32500 M^{-1}cm^{-1}$) at the maxima peak of absorption (475nm) (BD Living Colors-Clontechiques, 2005) was used.

Fluorescence measurements were carried out using a Jasco FP6500 spectrofluorometer in which the λ_{ex} was fixed at 465 nm. Emission and excitation bandwidths were 3 nm.

The solutions of $Cd(NO_3)_2$, $Pb(NO_3)_2$, $Ni(NO_3)_2$ and $Cu(NO_3)_2$ for ICP Standard 1000mg/L (MERCK) were dissolved in Milli-Q water and were filtered with a Minisart filter (0.80µm). The absorption and emission spectrum in the same conditions were recorded.

To value that the effect was determined by metal ion respect the nitrate, different solutions of copper were used ($CuCl_2$, $CuSO_4$).

Then the analysis of spectroscopic characteristics of rAcGFP and of metal solutions, increasing amount of metals at the protein were added. After 5 min the absorption spectrum was measured while the emission spectrum after 10 min. The same volume of different metals was added (from 4 µl to 84 µl).

The Cary Eclipse Fluorescence spectrophotometer (Varian) was used only to obtain the fluorescence emission profiles of rAcGFP with copper (band widths excitation 5 nm, band width emission 5nm, scan control slow, scan rate 120 nm/min, averaging time 0.5 sec, data interval 1 nm) but the data were normalized to compare the results that we obtained using the two spectrofluorometers.

In the study of the behaviour fluorescence rAcGFP in presence of metal solutions the emission range from 470 nm to 600 nm was considered (λ_{ex} 465nm).

The emission spectra were normalized rather the absorption spectra to correct the dilution error when metals were added at the sample (fig. 13, 14).

Moreover, to determine the effective quenching effect, the normalization rather the maximum intensity emission of protein was elaborated.

The relative quenching was calculated as the change in fluorescence upon addition of metal ions relative to the no quenched fluorescence.

In order to evaluate possible matrix effects induced by NO_3^- and Cl^- ions, absorption and emission spectra of HNO_3 and NaCl were measured but some matrix effects did not find.

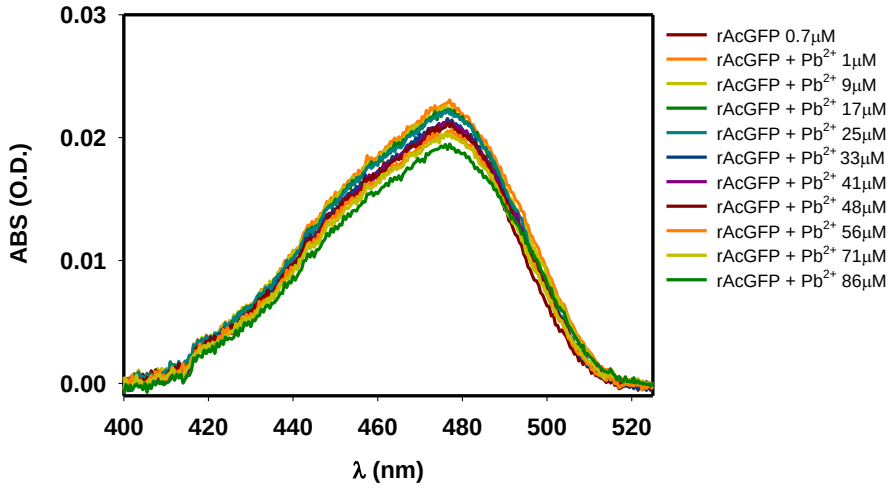

Fig. 13. Characteristic absorption spectrum of rAcGFP with Pb^{2+}.

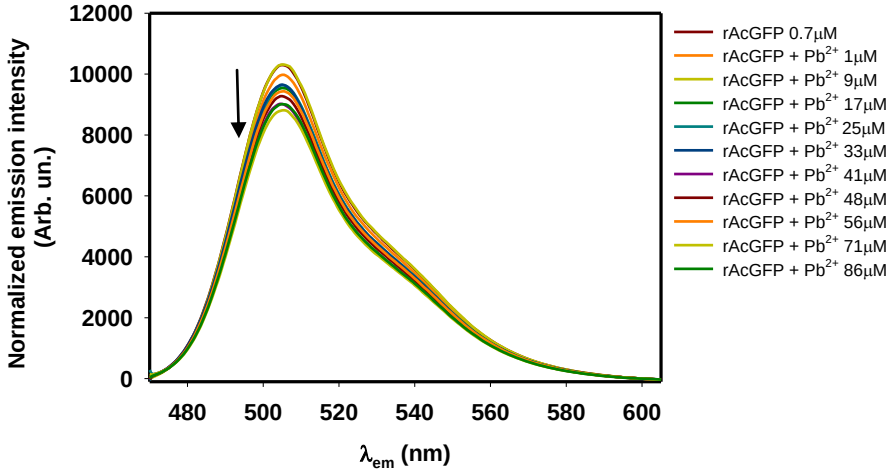

Fig. 14. Characteristic emission spectrum of rAcGFP with Pb^{2+}. These values are normalized rather the absorption at 465 nm. The arrow shows the decline of emission intensity when increasing concentration of lead are added.

2.3. Results and discussion

2.3.1. rAcGFP spectroscopic characterization

The figure 15 shows the range of absorption of rAcGFP in which there are two peaks. The first at 280 nm is the tryptophan peak while at about 465 nm there is the absorption peak of rAcGFP (Gurskaya *et al*., 2003).The concentration of rAcGFP was 0.7 µM (an error of 5% is attributed at this measure).

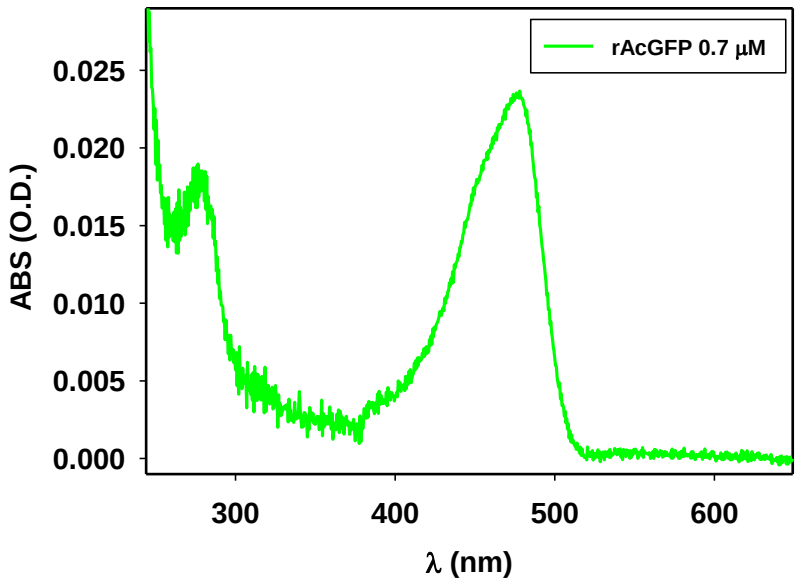

Fig. 15. Absorption spectrum of rAcGFP. Range from 250 nm to 650 nm.

Then, the attention was focused on the emission of rAcGFP. In figure 16 the emission spectra of protein rather at the change of excitation wavelengths are shown. The emission band shape, the position of emission peak and the intensity of fluorescence are valued.

The excitation wavelengths in the UV and visible range are used. The shape of band is unmodified by the excitation wavelength. Moreover, the position of emission peak at 500 nm was unmodified with the different excitation wavelengths while the emission intensity of protein was higher with λ_{ex} 465 nm rather the other wavelengths. So in all

assays this excitation was used. The excitation spectrum confirmed that the maximum excitation intensity is at about 465 nm if the emission wavelengths at 505 nm, 540 nm and 555 nm are used (fig. 17).

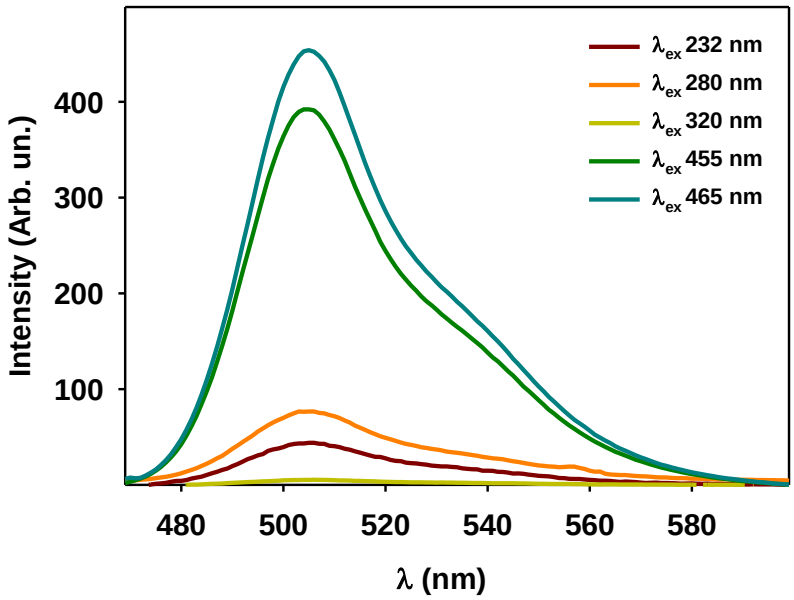

Fig. 16. Emission spectra of rAcGFP with λ_{ex} 232 nm, 280 nm, 320 nm, 455 nm and 465 nm. Range of emission from 470 nm to 610 nm.

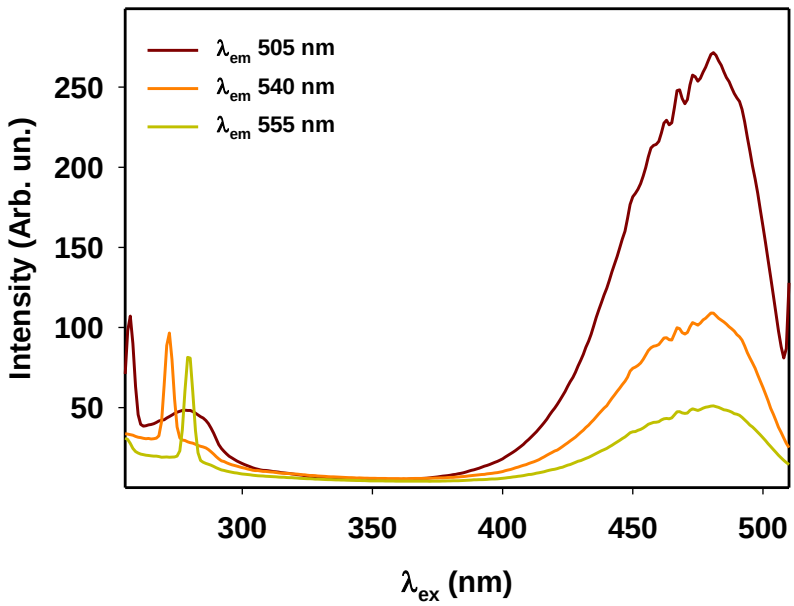

Fig. 17. Excitation spectra of rAcGFP with λ_{em} 505 nm, 540 nm, 555 nm. Range of excitation from 250 nm to 505 nm.

A summary of previous results is shown in the 3D spectrum (fig. 18). The excitation wavelengths from 423 nm to 523 nm with an increment of 5 nm are used. The increment of the excitation wavelength determines an increase of emission intensity but the position of the peak at 500 nm and the band shape are unmodified.

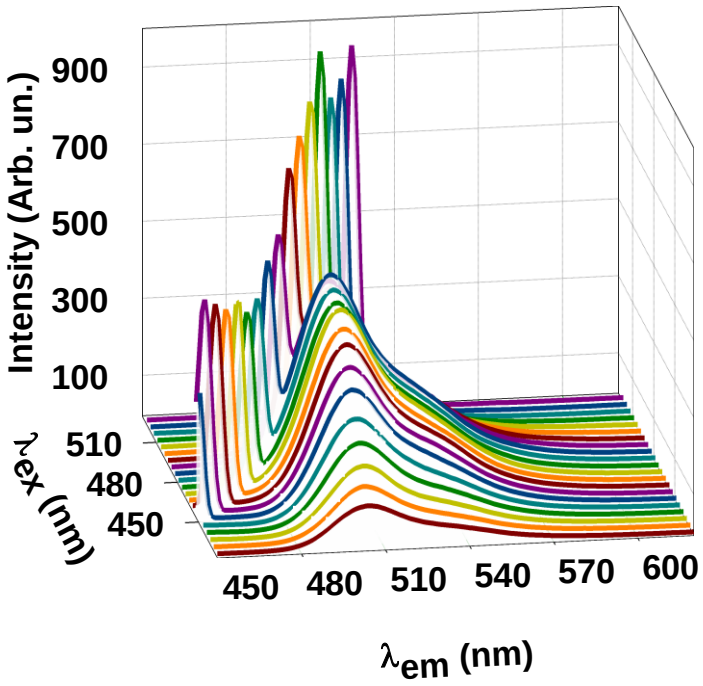

Fig. 18. 3D spectrum of rAcGFP. Range of excitation from 423 nm to 523 nm; range of emission from 450 nm to 620 nm.

The figure 19 shows the same results in which the emission band of the sample is visualized as a contour plot. The different colours represent the intensity of emission that is modified in function of the excitation wavelength. It is evident, as at $\lambda_{ex} < 440$ nm the emission intensity contribute of the peak at 505 nm is lower rather the next excitation wavelength. When the sample is excited with wavelengths from 460 nm to 475 nm there is the maximum emission, while at $\lambda_{ex} \geq 475$ nm the fluorescence intensity is near the saturation. The dashed lines show as the position of the peak is unmodified by the different excitation wavelengths.

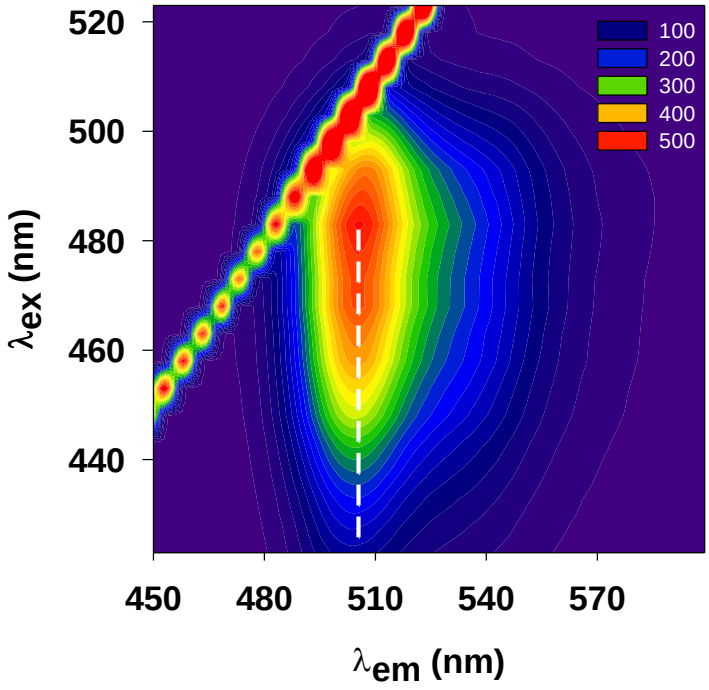

Fig. 19. Contour plot of rAcGFP. Range of excitation from 423 nm to 523 nm; range of emission from 450 nm to 620 nm.

2.3.2. Metals solutions spectroscopic characterization

The absorption spectrum of metal solutions was measured. $Cd(NO_3)_2$, $Pb(NO_3)_2$, $Ni(NO_3)_2$, $Cu(NO_3)_2$ showed an absorption at ~ 300nm, and only Ni^{2+} solution had a peak at ~ 400nm (fig. 20).

The emission spectrum of these solutions is measured but no fluorescence was observed (data not shown).

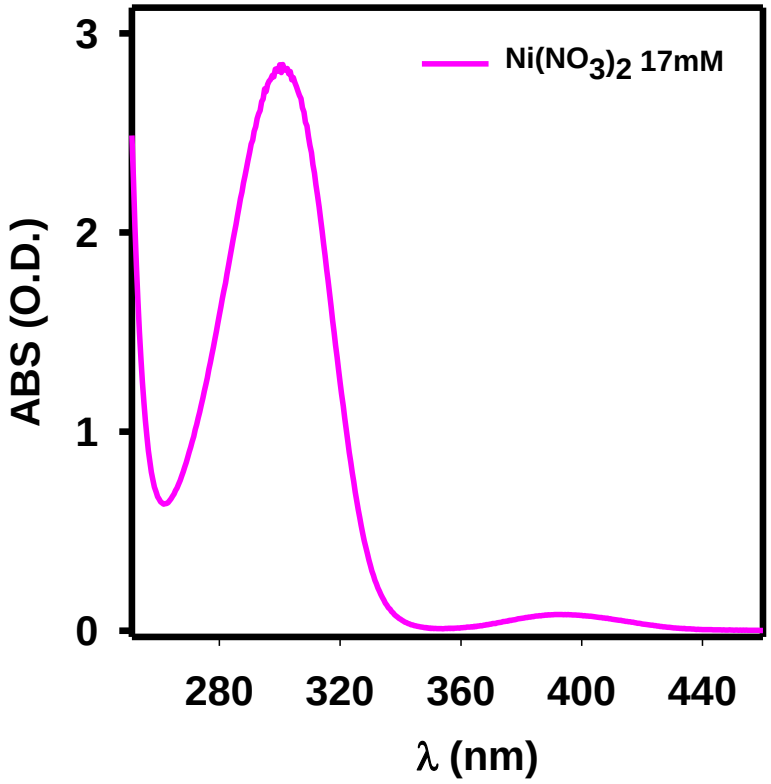

Fig. 20. Absorption spectrum of $Ni(NO_3)_2$. Range from 250 nm to 460 nm.

2.3.3. rAcGFP with metals spectroscopic characterization

In all assays, the maxima intensity of fluorescence is measured when no metal was added at the protein while a quenching of fluorescence occurred when we incremented metal concentration. The quenching was calculated by determining % fluorescence, which is the difference of the fluorescence at a given metal concentration divided by the fluorescence with no metal present. The error of these measures was esteemed about 5% and included the dilution error, the instruments error and the error of operator. The dilution error was calculated through the addiction of maxima volume of water (84 µl) at the sample in the same condition that we used for metals.

The figure 21 shows the evolution of quenching of rAcGFP fluorescence in presence of nickel (range of concentration from 0 to 475 µM). No sample precipitation occurred in presence of higher metal concentrations. Moreover, nickel does not seem to influence the fluorescence emission of GFP. The quenching effect at the maximum nickel concentration was of 14% (table 3).

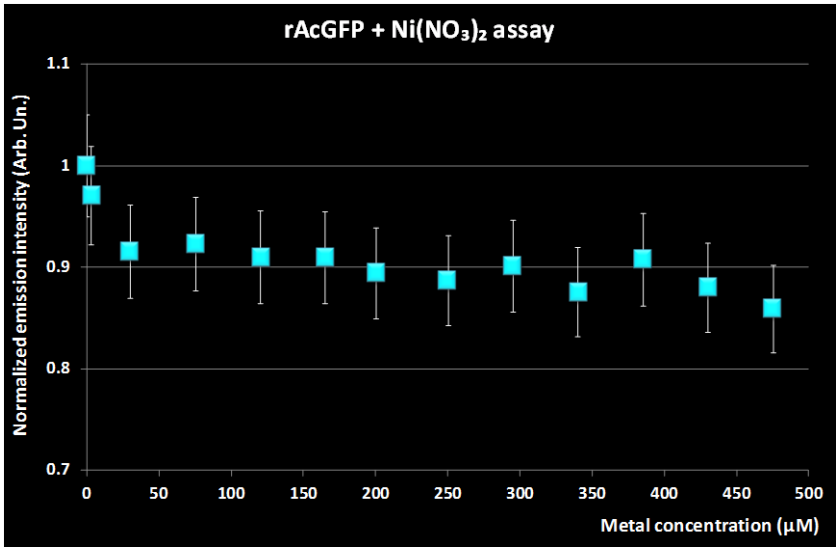

Fig. 21. Evolution of quenching of rAcGFP by nickel solution.

In figure 22 the evolution of quenching of rAcGFP fluorescence in presence of lead (range of concentration from 0 to 86 µM) is shown. Lead influenced the fluorescence emission of GFP rather nickel. In fact, the quenching effect at the maximum nickel

concentration was of 14% while this value for lead was at less significant concentrations (table 4).

Ni^{2+} concentration (µM)	*Emission (Arb. Un.)*	*% Quenching*
0	1	0
3	0.971	3
30	0.916	8
75	0.923	8
120	0.910	9
165	0.910	9
200	0.895	11
250	0.887	11
295	0.902	10
340	0.876	12
385	0.908	9
430	0.880	12
475	0.859	14

Table 3. Range of nickel concentrations used in the rAcGFP assays. Normalized emission values and quenching percentage at specific concentrations of metal.

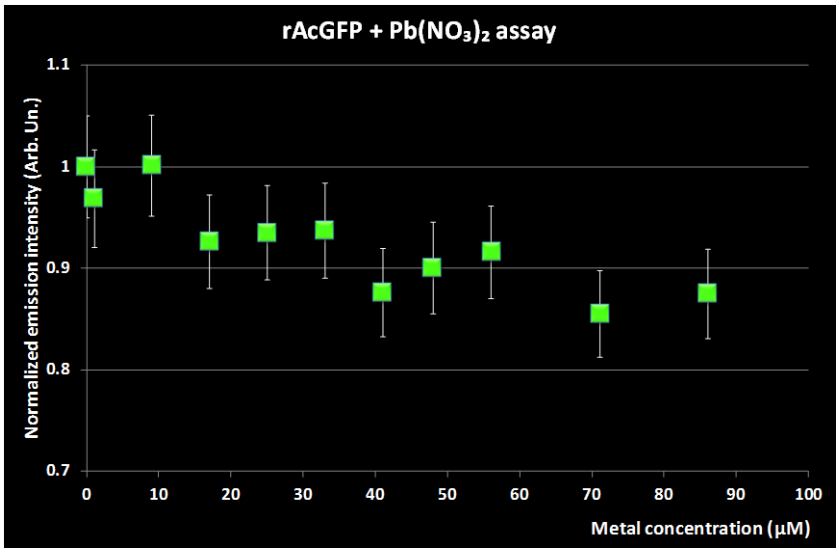

Fig. 22. Evolution of quenching of rAcGFP by lead solution.

Pb^{2+} concentration (μM)	Emission (Arb. Un.)	% Quenching
0	1	0
1	0.969	3
9	1.002	0
17	0.927	7
25	0.935	6
33	0.938	6
41	0.876	12
48	0.901	10
56	0.916	8
71	0.856	14
86	0.875	12

Table 4. Range of lead concentrations used in the rAcGFP assays. Normalized emission values and quenching percentage at specific concentrations of metal.

In figure 23 the evolution of quenching of rAcGFP fluorescence in presence of cadmium (range of concentration from 0 to 122 μM) is shown. Cadmium caused the quenching effect on the fluorescence emission of rAcGFP of 16% at the higher concentration (table 5).

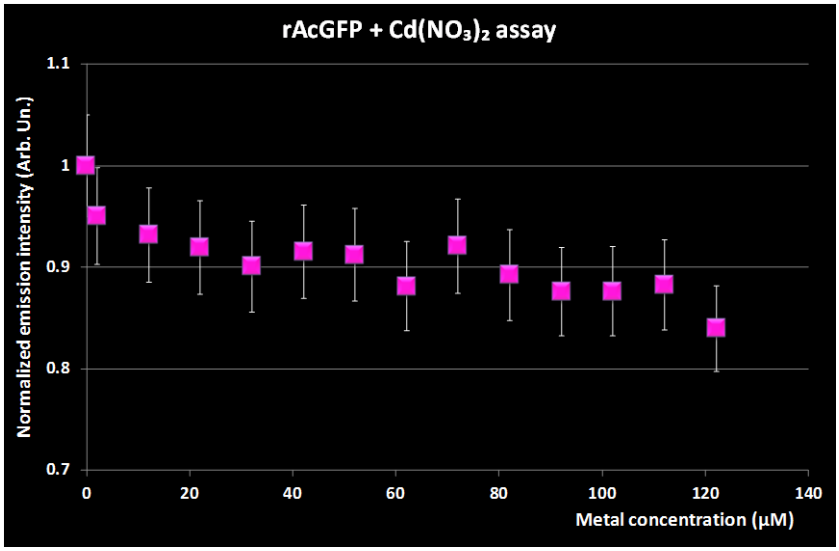

Fig. 23. Evolution of quenching of rAcGFP by cadmium solution.

Cd ²⁺ concentration (µM)	*Emission (Arb.Un.)*	*% Quenching*
0	1	0
2	0.951	5
12	0.932	7
22	0.920	8
32	0.901	10
42	0.916	8
52	0.913	9
62	0.882	12
72	0.921	8
82	0.893	11
92	0.876	12
102	0.877	12
112	0.883	12
122	0.840	16

Table 5. Range of cadmium concentrations used in the rAcGFP assays. Normalized emission values and quenching percentage at specific concentrations of metal.

In figure 24 the evolution of quenching of rAcGFP fluorescence in presence of copper (range of concentration from 0 to 65 µM) is shown. Copper influenced the fluorescence emission intensity of protein but the evolution of this effect shows quenching value fluctuations with the metal concentration (table 6). In presence of copper, a recovery of fluorescence through the addiction of EDTA (0.1M) at the sample was observed (data not shown).

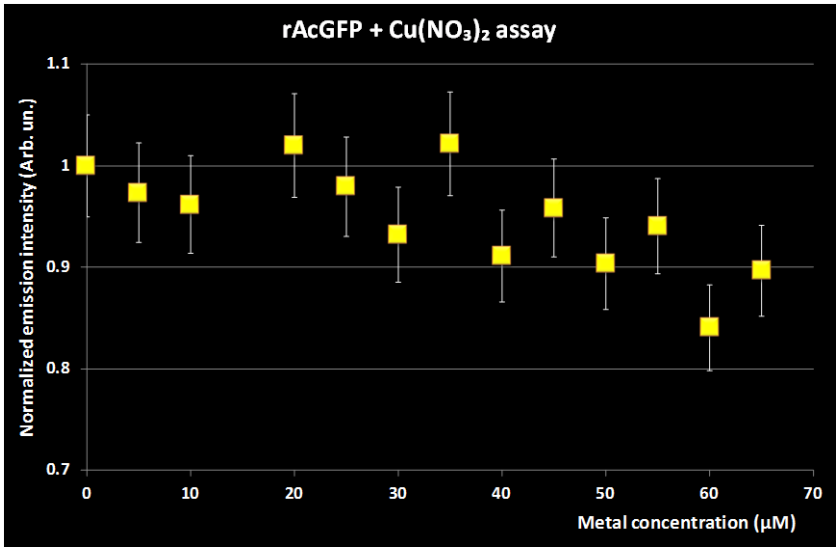

Fig. 24. Evolution of quenching of rAcGFP by copper solution.

Cu^{2+} concentration (μM)	Emission (Arb. Un.)	% Quenching
0	1	0
5	0.974	3
10	0.962	4
20	1.020	0
25	0.980	2
30	0.932	7
35	1.022	0
40	0.912	9
45	0.959	4
50	0.904	10
55	0.941	6
60	0.841	16
65	0.897	10

Table 6. Range of copper concentrations used in the rAcGFP assays. Normalized emission values and quenching percentage at specific concentrations of metal.

A summary of previous data are shown in figure 25. Quenching effects observed are different for investigated metals, having larger fluorescence decrease for Cu^{2+} and Pb^{2+} rather Ni^{2+} and Cd^{2+} (at about the same metal concentration).

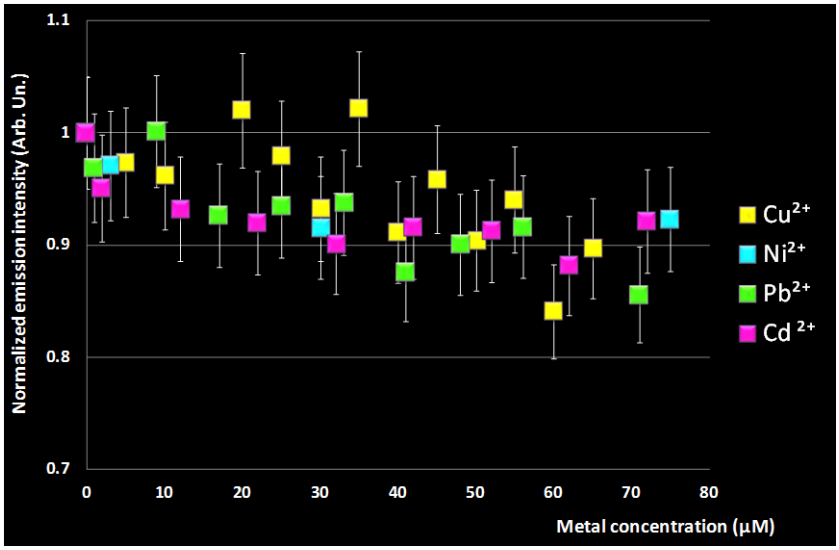

Fig. 25. Summary of rAcGFP quenching evolution in presence of all metals solutions.

To value if there were differences in the quenching of fluorescence in presence of copper with other anions the same experiments using $CuSO_4$ and $CuCl_2$ were conducted. The contribute of the anions in the quenching effect determined by copper [16 µM] was the same (fig. 26).

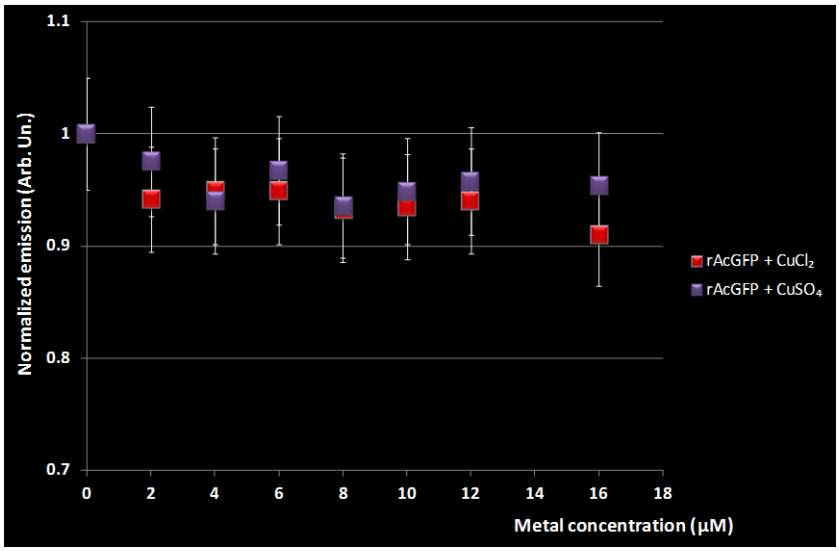

Fig. 26. Summary of rAcGFP quenching evolution in presence of $CuCl_2$ and $CuSO_4$.

Results of modest quenching that it is obtained for rAcGFP with Cu^{2+} was similar at results that Richmond *et al*. showed for the *wt* GFP in a report of 2000 and that Eli *and* Chakrabartty (2006) found for EGFP.

The emission stability of rAcGFP in presence of Ni^{2+} was measured in a range of temperature from 20 °C to 60 °C with a jump of 1°C every 2 min (fig. 27). The increase of temperature determines the protein precipitation and the decline of the emission intensity with a red shift of the peak at 500 nm of ~ 5 nm.

The absorption stability of protein was measured through about 50 cycles repeated of absorption measures at RT over night of rAcGFP with Cu^{2+}. No protein precipitation was observed (data not shown).

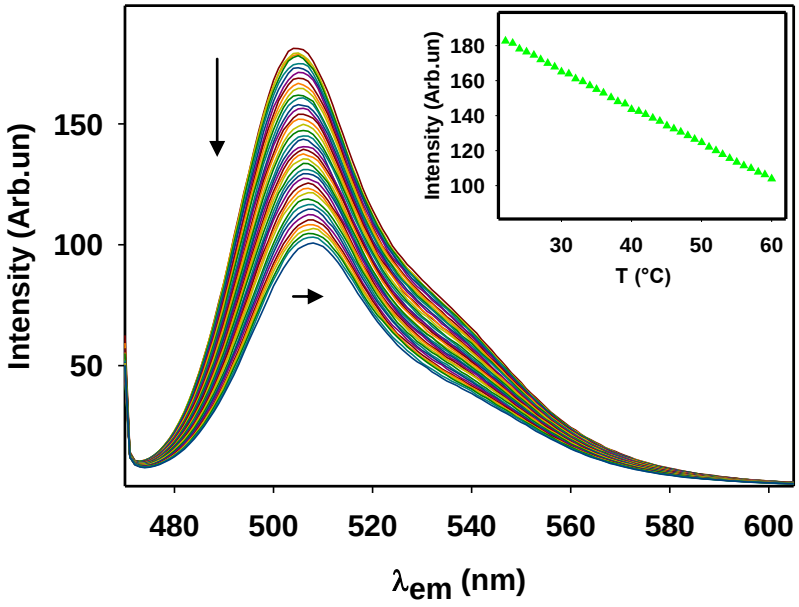

Fig. 27. Emission spectrum of rAcGFP with Ni^{2+} at diverse temperatures (from 20 °C to 60 °C). In the inset: profile of fluorescence intensity evolution at different temperatures.

2.4. Conclusions

In this study, the spectroscopic properties of a recombinant GFP from *A. coerulescens* were investigated. Moreover, the fluorescence protein behaviour in presence of environmental contaminants as cadmium, nickel, lead and copper potentially dangerous for human health, was analyzed.

A. coerulescens was selected among the others proteins because it derived from a cnidarian species as *A. sulcata* but it was a recombinant and a pure protein. rAcGFP was considered the control system to compare results obtained on the GFP that was extracted from *A. sulcata* and was partially purified according to the gel filtration.

The evolution and the value of quenching effect on the fluorescent emission of rAcGFP for all metals investigated, were the same. In fact, the metal – protein bond did not seem to be selective. The bond effect unchanged with the different metals investigated.

However, results did not highlight great differences of metals effects on the fluorescence intensity, they allowed to choose and select the best possible condition of assays (buffer solution, concentration, pH, temperature) acquiring the spectroscopic techniques.

3. Identification and characterization of Green Fluorescent Protein (GFP) from *Anemonia sulcata* (Forskal, 1775) and its environmental applications

3.1. Biology of Anemonia sulcata

One of the characteristic Mediterranean hard substrate assemblage are the dense colonies of the sea anemone *A. sulcata* (fig. 28) that being a component of the biocoenosis of the photophilic soft algae (Peres, 1982).

Fig. 28. *Anemonia sulcata*.

Its retractile tentacles are green color with purple tips that hold the symbiotic algae "zooxanthellae". Under normal conditions, this relationship is well protected; however, some events such as pathogenic contamination and exposure to excessive UV radiation damage this relationship. For example, excessive subjecting to UV radiation results in the overproduction of reactive oxygen species by algae in the anemones, and then the relationship is broken and this event is known as "bleaching". On the other hand, cold shock, pathogenic infections, and reduced salinity might also be other factors for bleaching (Leutenegger *et al*., 2007). On average the anemone is 8 cm large.

Anemones lives in the same substrate until the conditions become unsuitable, in this case, using a flexing motions the organisms swim to a new location. This species is extremely adaptable to various conditions of temperature and salinity.
The sexes are separate in some species while others are protandric hermaphrodites. Both reproductions can occur. In sexual reproduction, the sperm released through the mouth, stimulate the release of eggs, so the fertilization occurs. The egg develops into a planula, which grows into a polyp. The asexual reproduction occurs through extratentacular budding.

3.2. Materials and methods

3.2.1. Sample collection and confocal microscopy analysis

Several specimens of *A. sulcata* were collected from a depth of 0.5 m along a bay near Sciacca (Sicily). Then, the anemones were transferred promptly to aerated tanks with natural seawater in laboratory and the tentacles were cut at the basis.
A tentacle of *A. sulcata* was placed on microscope slides with 0.5 ml of water and imaged using a Leica RCS SP5 confocal laser scanning microscope with a 63x oil objective NA = 1.4 (Leica Microsystems, Germany) with a scanning frequency of 400 Hz. 1024x1024 images were acquired using a 476 nm line of an argon laser as excitation and the emission spectral range was set from 490 nm to 600 nm and from 635 nm to 780 nm, pin hole was 95mm.

3.2.2. Protein extraction assay

The samples (tentacles) were homogenized in Triton 1%, PBS and a protease inhibitor cocktail (AEBSF, Aprotinin, Bestatin, E 64, Leupeptin and Pepstatin A) (Sigma-Aldrich) using a glass potter homogenizer. Then samples were centrifuged at 10,000 rpm for 10 min at 4°C in order to remove the cell debris. After, the surnatant was used to repeat another cycle of centrifugation at the same conditions. The total protein concentration on the surnatant was measured using a Bio-Rad Protein Assay (Bio-Rad).

Bovine Serum Albumin (BSA) (Sigma-Aldrich) was used for generating accurate standard curve of absorption (595nm) in function of concentration.

3.2.3. Sodium dodecyl sulphate - polyacrylamide gel electrophoresis (SDS-PAGE)

Surnatant was dissolved in Sample buffer 6X (SDS 10%, Tris 0,5 M at pH 6,8, glycerol, Bromophenol blue 0.1%, Milli-Q water). Then, it was loaded on a 10% polyacrylamide gel (acrilamide / N,N'-metilenbisacrilamide 30 % : 0.8%, Tris-HCL 1,5 M at pH 8.8, Tris-HCL 0,5 M at pH 6.8 , Milli-Q water, SDS 10%, APS and TEMED; running buffer 10X: Tris-Glycine, SDS, Milli-Q water) both in non/reducing conditions. To reduce the sample, β-mercaptoethanol was added to the sample and after was boiled for 5 min. Comassie Brilliant Blue 250G (Sigma-Aldrich) was used for staining protein in the denatured sample. Then, the image of the destained gel was acquired on a flatbed scanner. Moreover, the same gel was imaged at Versa-Doc Imaging System (Bio-Rad) using a FITC fluorophore with a 530BP blue led to detect a fluorescent protein. This instrument allowed to see the fluorescent bands on gels on in others substrates when fluorescent sample were loaded.
Molecular Weight Marker (36 – 205 KDa) and Fluorescent Molecular Weight Marker (20.1 – 205 KDa) were used to as a size standards.

3.2.4. Gel filtration and HPLC

To obtain a partially purified protein solution, the raw extract was used in a Gel Filtration experiment. Sephadex G75 (3000 – 80000 Da) (Pharmacia) was used as stationary phase while 4-Morpholineethanesulfonic acid hydrate (MES) 20mM pH 7 was used as eluent phase (before it was filtered with a filter of 0.80µm). Injection volume of raw extract was 700µl, flow rate was 0.5ml min^{-1} while 1ml of the fractions were collected with a collector (Amersham Pharmacia).
HPLC with a stainless steel column (50mm X 300mm) was performed to value the grade of purification of fluorescent fractions obtained from Gel Filtration with Sephadex G75.

Sephadex G200 (5000 – 600000 Da) (Pharmacia) was used as stationary phase while 4-Morpholineethanesulfonic acid hydrate (MES) 20mM pH 7 was used as eluent phase. Loop of raw extract was 20µl, flow rate was 1ml min^{-1} while ABS was fixed at 254nm. Alcohol deidrogenase (150KDa), BSA (66 KDa) and anhydrase carbonic (29KDa) were used as standards.

3.2.5 Spectral analysis of partially purified sample and metal solutions

Partially purified protein was dissolved in MES 20mM (1:5) solution at pH 7 and filtered with a Minisart filter (0.80µm) (Sartorius). A UV-Vis recording spectrophotometer (Shimadzu) with a 1cm path length cuvette was used for absorbance spectra measurements in a range from 190 nm to 900 nm (scan speed: medium; sampling interval: 0.5). The partially purified protein concentration was determined using Beer-Lambert law. The concentration of isolated AsGFP was 0.1 µM (an error of 5% is attributed at this measure). It was calculated using the molar coefficient extinction ($88000 M^{-1}cm^{-1}$) at the maxima peak of absorption (480nm) that Tasdemir *et al*. (2008) used in their report. The Cary Eclipse Fluorescence spectrophotometer (Varian) was used to obtain the fluorescence emission profiles of sample (band widths excitation 5 nm, band width emission 5nm, scan control slow, scan rate 120 nm/min, averaging time 0.5 sec, data interval 1 nm) by exciting at different wavelengths. The λ_{ex} was fixed at 270 nm, 290 nm, 300 nm, 380 nm and 460 nm. The Jasco FP 6500 Spectrofluorometer was used to obtain the fluorescence excitation profiles ($BW_{\lambda ex}$ 3, $BW_{\lambda em}$ 3) in which the λ_{em} was fixed at 320nnm, 350nm and 360nm.

Metal solutions $Cd(NO_3)_2$, $Pb(NO_3)_2$, $Ni(NO_3)_2$, $Cu(NO_3)_2$, were diluted in Milli-Q water and were filtered with a Minisart filter (0.80µm). The absorption and emission spectrum in the same conditions were recorded.

Then, increasing amount of metals at the protein were added. So, the attention was focused on the fluorescence emission behaviour of AsGFP using only the emission spectrum with λ_{ex} 460nm and 300nm. After 5 min the absorption spectrum was measured while the emission spectrum after 10 min. The same volume of different metals was added (from 4 µl to 84 µl).

Some metals showed for the last concentrations an increment of scattering and absorption at the different peaks of sample (fig. 29). So, the absorption spectrum was used to value this aggregation phenomenon and when aggregation occurred, the emission results at specific metal concentration did not consider.

The fluorescent intensity was recorded directly at the corresponding emission maxima peaks of protein. The relative quenching was calculated as the change in fluorescence upon addition of metal ions relative to the no quenched fluorescence. The experiments were done in two replicates.

In order to evaluate possible matrix effects induced by NO_3^- and Cl^- ions, absorption and emission spectra of HNO_3 and NaCl were measured but some matrix effects did not find.

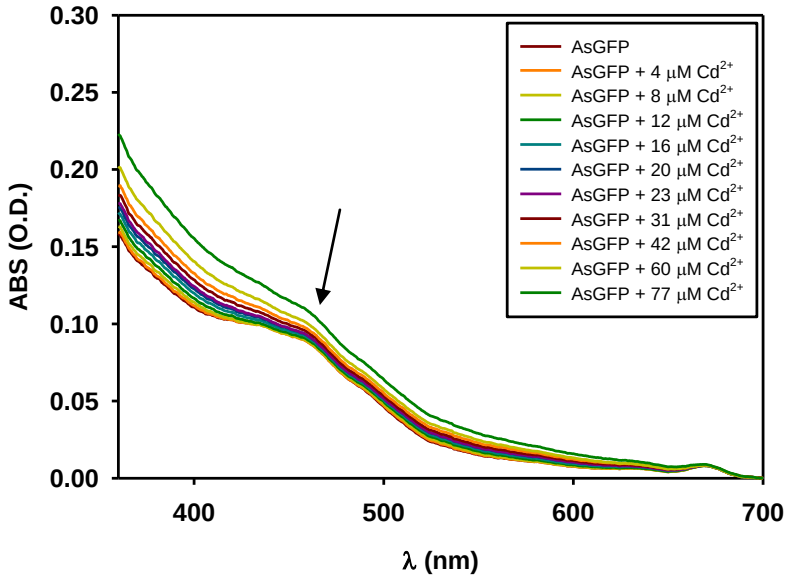

Fig. 29. Absorption spectrum of partially purified sample with Cd^{2+} (range of concentration from 4 to 77 µM). ABS range from 380 nm to 700 nm. The scattering is indicated by the arrow.

3.2.6. Dot Blot assay

Partially purified protein was spotted through circular template on ECL Hybond Nitrocellulose membrane (Amersham). Many dilutions of sample in MES 20mM at pH7

were used. Moreover, different acquisition times for the quantitative analysis were considered. Versa-Doc Imaging System (Bio-Rad) was used to acquire the fluorescent bands on the gel. ChemiDoc (BIORAD) was used to quantify the fluorescence bands. Increasing concentrations of Cu^{2+} (from 20 µM to 120 µM) were added to 100 nM of AsGFP. After 10 min, the effect on the fluorescence intensity was detected.

3.3. Results

3.3.1. Confocal microscopy results

In figure 30A the sample of *Anemonia* in vivo using the Versa-Doc Imaging system is shown. The fluorescence is visualized only in the tentacles portion. The optic section of the tentacle is shown in figure 30B in which the presence of two species of fluorescent protein that are separated in two different portions of the tentacle is evident.

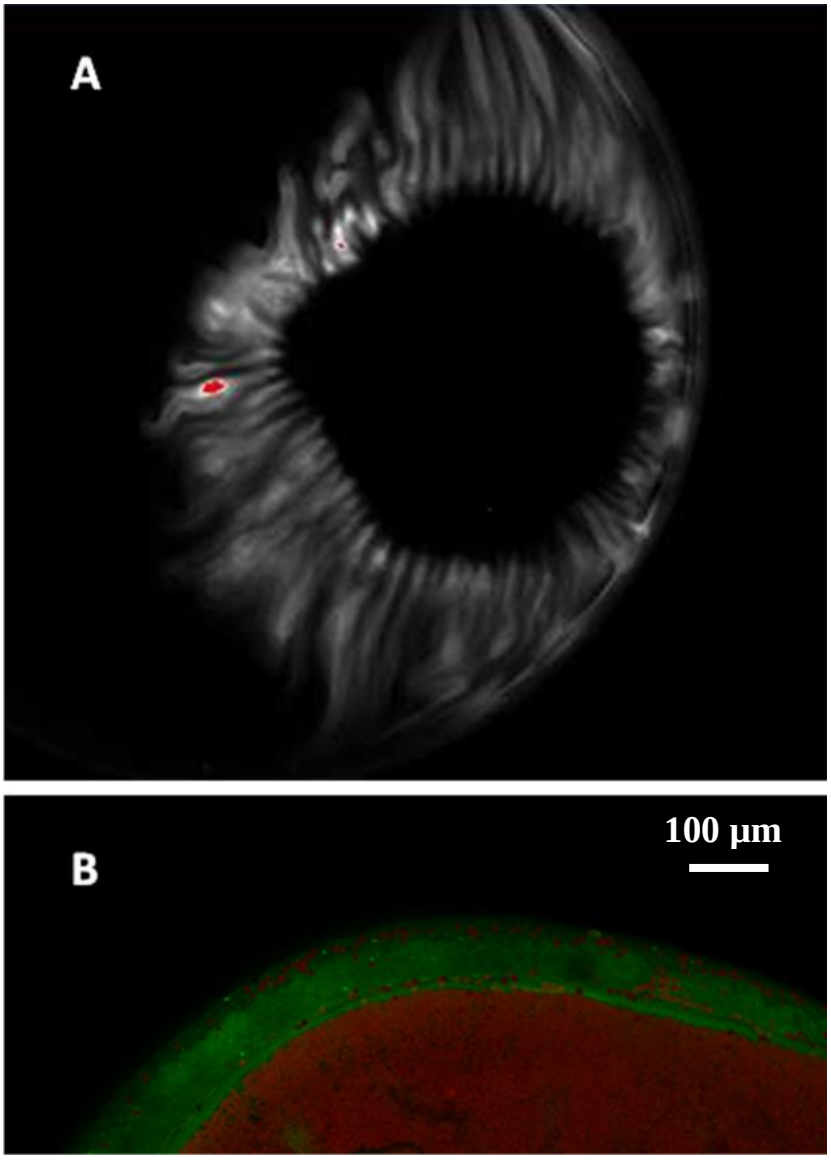

Fig. 30. A) *A. sulcata* in vivo (Versadoc imaging Systems, using FITC as fluorophore, blue led 530 BP). B) Optic section of the tentacle (Olympus 1X70 with Melles Griot laser system, 10X objective).

A particular of the interface region between the green (ectoderm portion) and red (gastroderm portion) fluorescence is shown in figure 31.

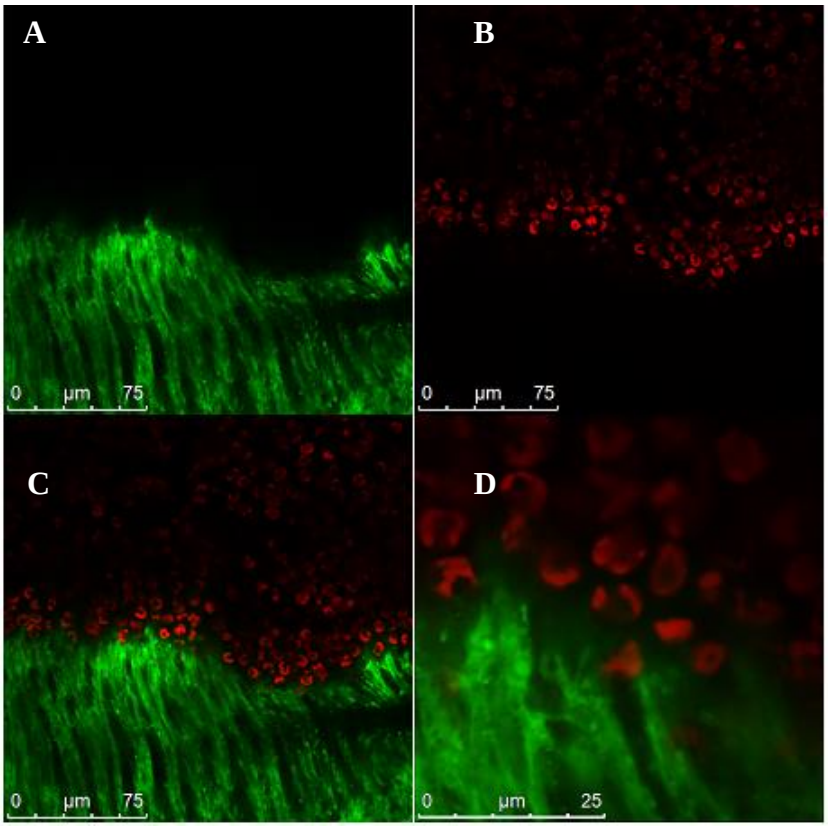

Fig. 31. Particular of the tentacle of *A. sulcata* (confocal imagine, 63X objective). A) Green fluorescence of the ectodermal region. B) Red fluorescence of gastrodermal region. C) Overlapping of the two region. D) Zoom of C.

The green fluorescence is shown in figure 32A. The emission spectrum of the area in the yellow circle is shown in figure 32E in which the excitation at 476 nm and the emission spectral range from 490 nm to 600 nm are used. This is the emission band of AsGFP. The red fluorescence is shown in figure 32B. The emission spectrum of the area in the yellow circle is shown in figure 32F in which the excitation at 476 nm and the emission spectral range from 635 nm to 780 nm are used. This is the emission band of chlorophyll that is present in the zooxantellae. The same imagine is shown using the transmission channel and all previous channels (fig. 32C/D).

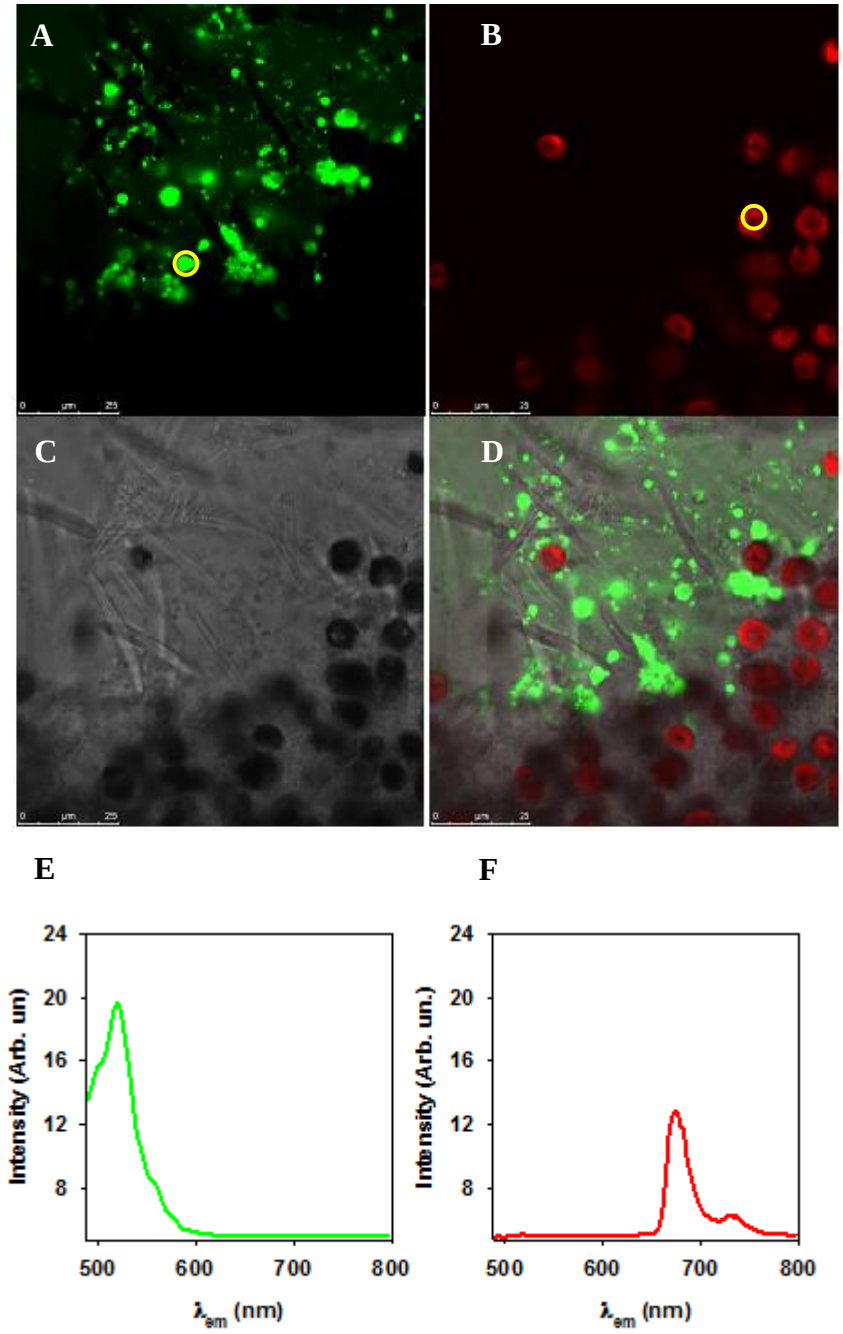

Fig. 32. Particular of the tentacle of *A. sulcata* (confocal imagine, 63X objective). A) Green fluorescence of the ectodermal region. B) Red fluorescence of gastrodermal region. C) Ectodermal and gastrodermal regions (transmission channel). D) The same region observed with all channels. E) Emission spectrum of the area in the yellow circle of A. F) Emission spectrum of the area in the yellow circle of B.

3.3.2. Biochemical characterization of partially purified sample

The concentration of raw extract was 17,5µg μl^{-1} according to the Bio-Rad Protein Assay (Bio-Rad).

SDS-PAGE 10% in no reducing condition is shown in figure 33A. The raw extract in different dilutions is loaded (1:2 and 1:4). This gel was imaged at Versa-Doc Imaging System (Bio-Rad). A single fluorescent band was present in all dilutions at ~ 116 KDa. Fluorescent Molecular Weight Marker (20,1 – 205 kDa) was used to compare the size of sample fluorescent band while the Molecular Weight Marker (36 – 205 KDa) did not show any bands. A molecular weight of ~ 124 kDa for the band of raw extract was calculated through the plot of the relative mobility (Rf) versus log MW of the standard.

When sample was overloaded (77 µg) a smear effect occurred (line 3). Whereas after a dilution of raw extract, the fluorescent band was more clear (line 4, 5).

The same raw extract was loaded on SDS-PAGE 10% in reducing conditions (fig. 33B). In this case β-mercaptoethanol was added at 23µg of raw extract and after it was boiled for 5 min. No fluorescent band was observed when the gel was imaged at Versa-Doc Imaging System while the protein patterns was obtained after coloration with Comassie Brilliant Blue 250G.

The Bio-Rad Protein Assay (Bio-Rad) was used to calculate the concentration of the proteins eluted after the gel filtration with Sephadex G75 of the raw extract.

The plot of concentration versus the elution time revealed that the greatest protein concentrations were recording after 15 min and within 30 min of elution (fig. 34). Among all the eluted fractions at the same concentration, only some of them showed a fluorescence. These were eluted from 20 min at 28 min, but the maxima fluorescence intensity was present in the eluted fractions from 22 to 24 min (fractions in the maxima peaks of profile).

In the figure 35 the protein pattern of the all previous fractions that were loaded on SDS-PAGE 10% is shown. The samples were reduced with β-mercaptoethanol and were boiled for 5 min. The raw extract was loaded on the gel after the centrifugation with Microcon YM-10 centriful filter unit (Sigma-Aldrich) too. The same concentration was used to load the different samples.

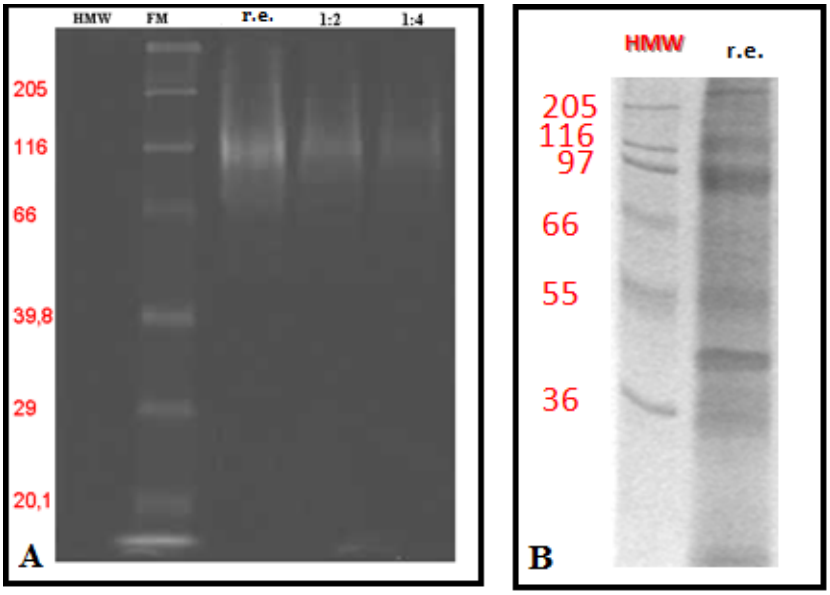

Fig. 33. A) SDS-PAGE 10% in no reducing conditions. Line 1: Molecular Weight Marker (36 – 205kDa); Line 2: Fluorescent Molecular Weight Marker (20,1 – 205 kDa); Line 3: raw extract; Line 4: raw extract diluted 1:2; line 5: raw extract diluted 1:4. B) SDS-PAGE 10% in reducing conditions. *Line 1:* Molecular Weight Marker (36 – 205 KDa); *Line 2:* raw extract [23µg].

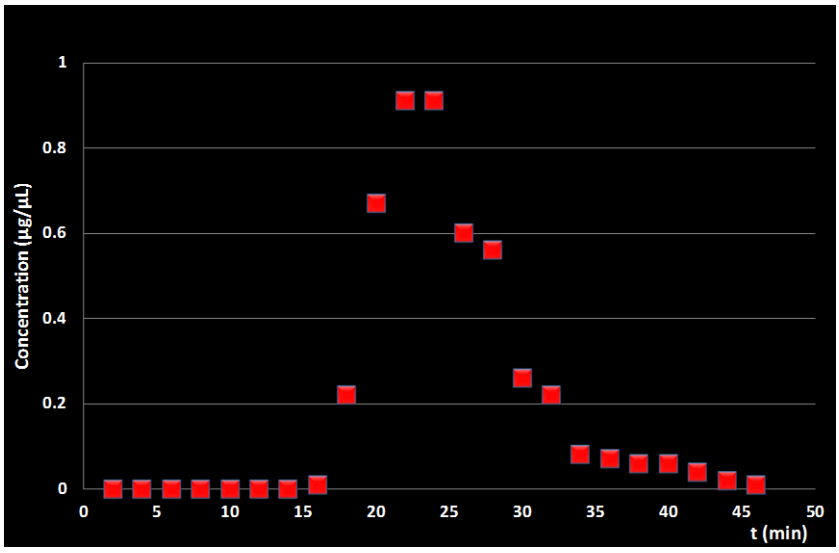

Fig. 34. Raw extract elution profile. X axis: time of elution (min), Y axis: concentrations of the fractions eluted through the gel filtration with Sephadex G75 (µg μl^{-1}).

All fractions that showed fluorescence and had the same protein patterns were added so this unique sample that we called “partially purified protein” (PPS), was used for the spectroscopic analysis.

HPLC assay on raw extract and on PPS with Sephadex G75 proved that the Bio-Rad Protein Assay determined an alteration of the real sample concentration while the raw extract concentration was similar at the concentration calculated through the peak area.

PPS was partially purified for the 80% rather the raw extract.

HPLC assay with Sephadex G 200 proved that only the 6.8% of PPS was the real fluorescent component.

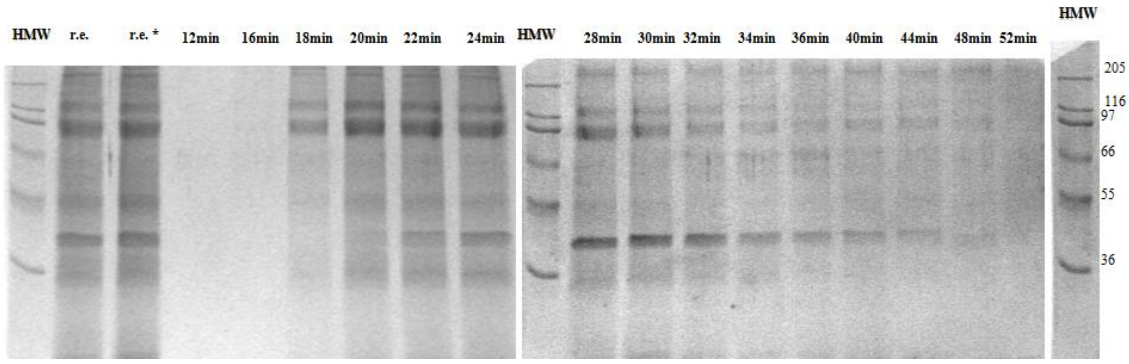

Fig. 35. SDS-PAGE 10% of the eluted fractions during the gel filtration on Sephadex G75 of the raw extract.
Line 1: Molecular Weight Marker (36 – 205 KDa); Line 2: raw extract; Line 3: raw extract *(after the filtration); Line 4: eluted after 12 min; Line 5: eluted after 16 min; Line 6: eluted after 18 min; Line 7: eluted after 20 min; Line 8: eluted after 22 min; Line 9: eluted after 24 min; Line 10: Molecular Weight Marker (36 – 205 KDa); Line 11: eluted after 28 min; Line 12: eluted after 30 min, Line 13: eluted after 32 min; Line 14: eluted after 34 min; Line 15: eluted after 36 min; Line 16: eluted after 40 min; Line 17: eluted after 44 min; Line 18: eluted after 48 min; Line 19: eluted after 52 min.

3.3.3. Spectroscopic characterization

3.3.3.1. Partially purified sample

The figure 36 shows the entire range of absorption of PPS in which there are many peaks. The first at 280 nm is the tryptophan peak while at 460 nm there is the absorption peak of AsGFP (Wiedenmann *et al*., 2000). At about 630 nm and 680 nm there are the chlorophyll absorption peaks (data not show) (Frigaard *et al*., 1996). In figure 37, a zoom of previous figure is reported, in which the AsGFP absorption peak is isolated. In fact, it is evident as near the peak at 460 nm there are many contribute of other bands that increase the effective absorption at this wavelength.

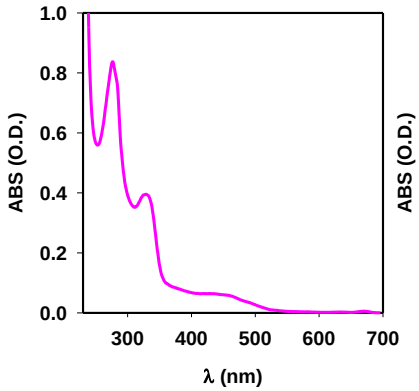

Fig. 36. Absorption spectrum of PPS, range from 230 nm to 700 nm.

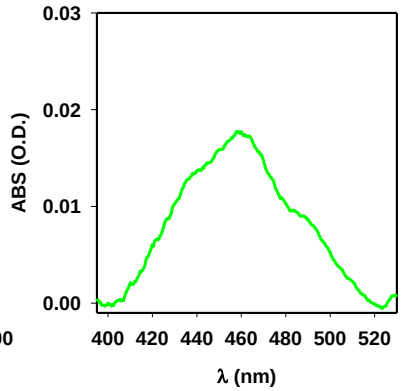

Fig. 37. Absorption spectrum of AsGFP, range from 395 nm to 525 nm.

Then, the attention was focused on the emission of the PPS.

In figure 38 it is shown the 3D spectrum of PPS in which the wavelength of excitation is changed and the emission band shape, the position of emission peaks and the intensity of fluorescence are valued. The excitation wavelengths from 370nm to 470nm with an increment of 10nm are used. In the emission range of AsGFP, the shape of band is modified by the excitation wavelength. In fact from 370 nm to 430 nm the higher intensity is determined by the peak at 500 nm. At λ_{ex} 440 nm, a modification of peaks ratio in which there is the same intensity contribute occurs. Instead, when λ_{ex} 470 nm an

increment of intensity at 518 nm occurs. The position of emission peaks both of AsGFP as of asFP595 and the chlorophyll are unmodified with the different excitation wavelengths. For this reasons the sample was excited at 460 nm. In this condition the maxima emission intensity at the two peaks of AsGFP was recorded and better the mutation of the peaks ratio was valued. Moreover, with λ_{ex} 460 nm it was possible to value the influence of the other peaks (asFP595 and Chl) when metals was added at the sample.

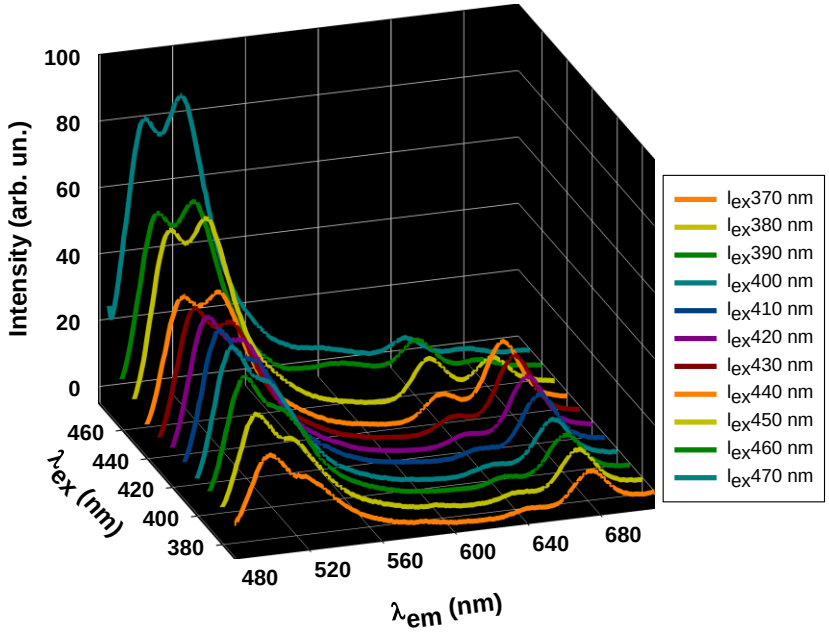

Fig. 38. 3D spectrum of PPS. Range of excitation from 370 nm to 470 nm, range of emission from 470 nm to 700 nm.

The figure 39 shows the same results in which the emission band of the sample is visualized as a contour plot. The different colours represent the intensity of emission that is modified in function of the excitation wavelength. It is evident, as at $\lambda_{ex} < 440$ nm the emission intensity contribute of the peak at 500 nm is higher than peak at 519 nm. When the sample is excited with wavelengths from 440 nm to 460 nm there is a equilibrium of the contribute of the two peaks, while at $\lambda_{ex} \geq 470$ nm there is an enhance of the emission intensity at 519 nm. The dashed lines show as the position of the two peaks is unmodified by the different excitation wavelengths.

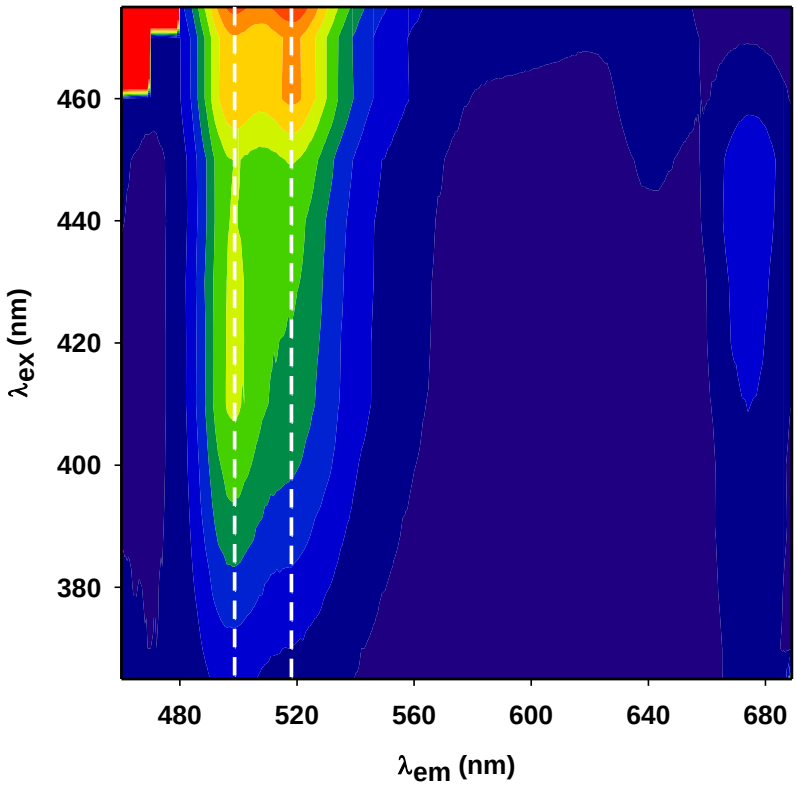

Fig. 39. Contour plot of PPS. Range of excitation from 370 nm to 470 nm. Range of emission from 470 nm to 690 nm.

The characteristic emission spectrum of PPS with λ_{ex} 460nm is shown in figure 40. Many bands of emission are present. The two peaks at 500 nm and 519 nm are the emission peaks of AsGFP (Wiedenmann *et al*., 2000). The third peak at 595 nm is the emission peak of asFP595 (Wiedenmann *et al*., 2000) while the next are the chlorophyll emission peaks.

In figure 41 as the ratio of the two emission peaks of AsGFP enhances with the increase excitation wavelengths is shown.

The stability of sample through about 80 cycles repeated of absorption measures at RT over night was measured but no protein precipitation was observed.

Then, the emission stability of sample through about 80 cycles of emission measures (λ_{ex} 460 nm) at RT over night was measured but no difference in the emission band shape and in the position of the peaks was detected.

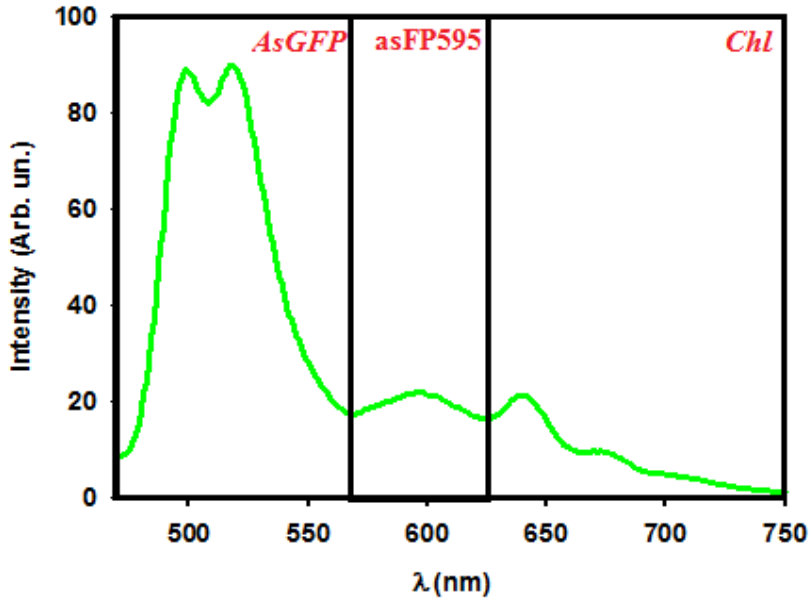

Fig. 40. Emission spectrum of PPS (λ_{ex} 460nm). Range of emission from 460 nm to 750 nm.

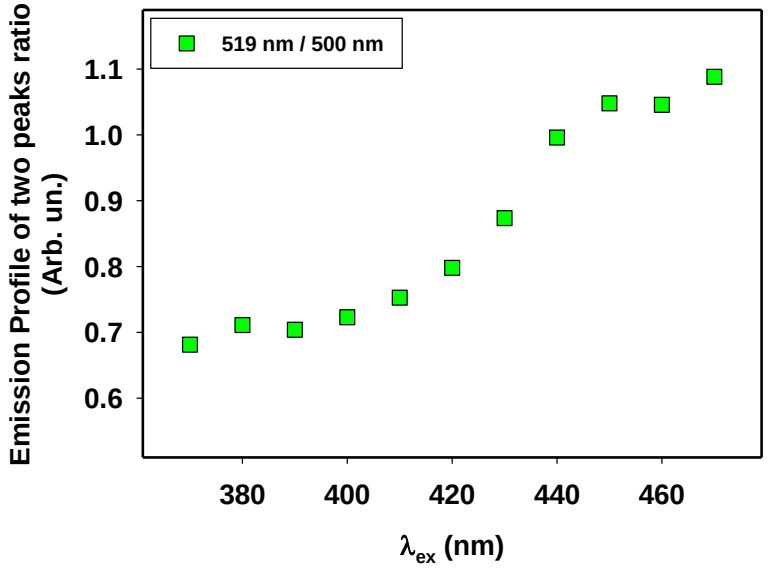

Fig. 41. Emission trend of ratio maximum intensity at 500 nm and 519 nm in function of different excitation wavelengths (range from 370 nm to 470 nm).

3.3.3.2. Metals solutions

The absorption spectrum of metal solutions was measured. $Cd(NO_3)_2$, $Pb(NO_3)_2$, $Ni(NO_3)_2$, $Cu(NO_3)_2$ showed an absorption at ~ 300nm, and only Ni^{2+} solution had a peak at ~ 400nm.

The emission spectrum of these solutions is measured but no fluorescence was observed (data not shown).

3.3.3.3. Partially purified sample and metals solutions

The characteristic emission spectrum of PPS in presence of copper is shown in figure 42.

In all assays "PPS – metals" any modification on the emission of asFP595 was observed. So, only the emission range from 470nm to 570nm for the study of the fluorescence AsGFP behaviour in presence of metal solutions was considered (fig. 43).

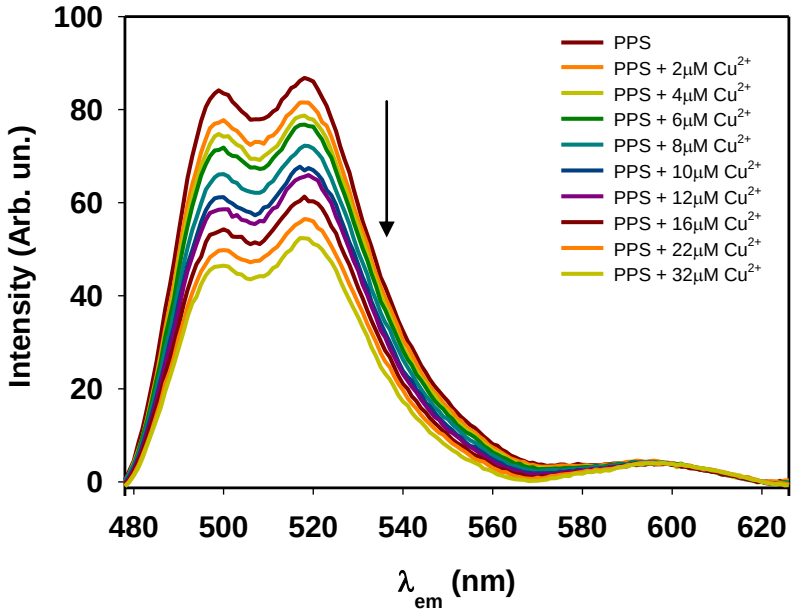

Fig. 42. Emission spectrum of PPS (λ_{ex} 460 nm) with Cu^{2+}. Range of emission from 470 nm to 630 nm. The arrow shows the decline of intensity fluorescence.

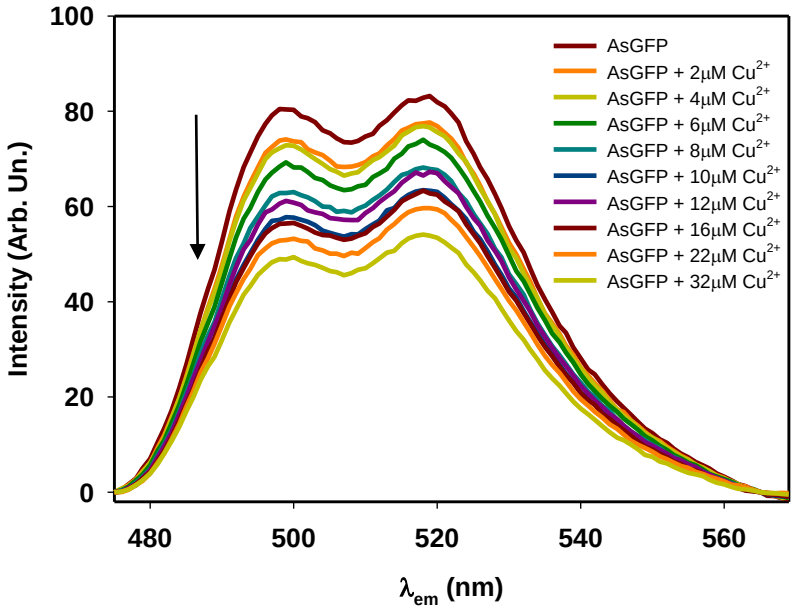

Fig. 43. Emission spectrum of AsGFP (λ_{ex} 460 nm) with Cu^{2+}. Range of emission from 470 nm to 565 nm. The arrow shows the decline of intensity fluorescence.

The maximum intensity of fluorescence is measured when any metal was added at the protein while a quenching of fluorescence occurred when we incremented metal concentration. The quenching was calculated by determining % fluorescence, which is the difference of the fluorescence at a given metal concentration divided by the fluorescence with no metal present.

Only the emission measures, in which there was not present protein aggregation or precipitation in the absorption spectrum, were considered.

In the analysis of Cu^{2+} effects on the AsGFP fluorescence intensity, a quenching about of 35% at 32 μM of copper was determined (fig. 44, table 7). The AsGFP fluorescence in presence of each metal is normalized for the maximum value of protein intensity when any metal is added. The error of measures was esteemed about 5% and included the dilution error, the instruments error and the error of operator. The dilution error was calculated through the addiction of maxima volume of water (84 μl) at the sample in the same condition that was used for metals. Moreover, in presence of copper, a recovery of fluorescence through the addiction of EDTA (0.1M) at the sample was observed.

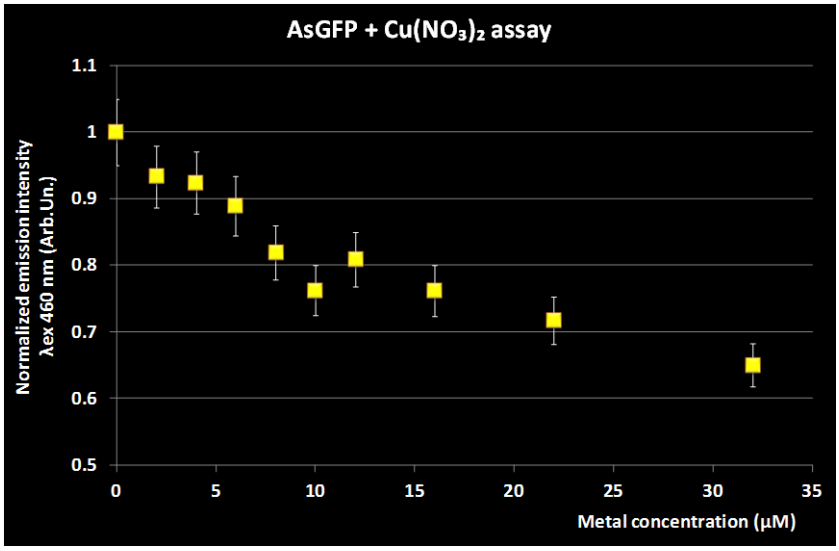

Fig. 44. Evolution of quenching of AsGFP by copper solution.

Cu^{2+} concentration (µM)	*Emission (Arb. Un.)*	*% Quenching*
0	1	0
2	0.933	7
4	0.924	8
6	0.890	11
8	0.819	18
10	0.762	24
12	0.809	19
16	0.761	24
22	0.717	28
32	0.650	35

Table 7. Range of copper concentrations used in the AsGFP assays. Normalized emission values and quenching percentage at specific concentrations of metal.

In figure 45 is shown the evolution of quenching of AsGFP fluorescence in presence of lead (range of concentration from 0 to 34 µM) (table 8). Lead influenced the fluorescence emission of GFP with a intensity decrement of 17% at 34 µM.

This quenching effect appeared less significant rather the copper decrement observed in the previous experiment.

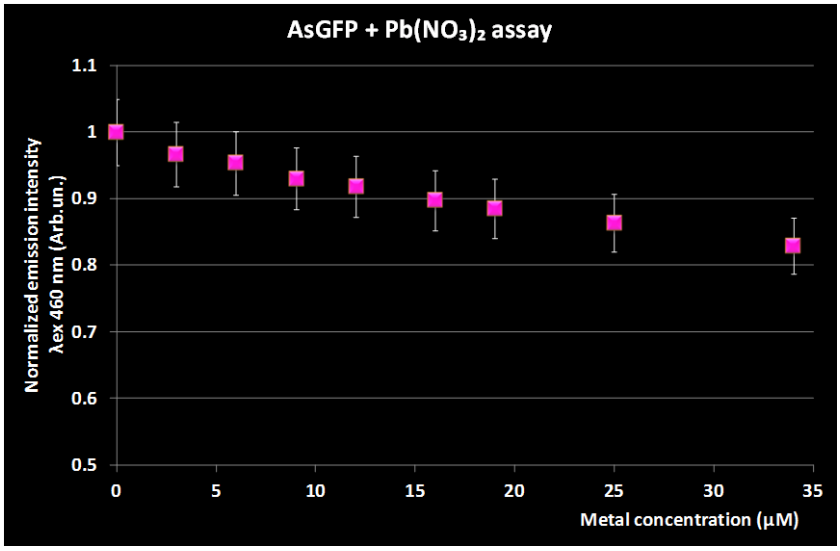

Fig. 45. Evolution of quenching of AsGFP by lead solution.

Pb^{2+} concentration (µM)	*Emission (Arb. Un.)*	*% Quenching*
0	1	0
3	0.967	3.3
6	0.954	4.6
9	0.930	7
12	0.918	8.2
16	0.897	10.3
19	0.885	11.5
25	0.864	13.6
34	0.829	17.1

Table 8. Range of lead concentrations used in the AsGFP assays. Normalized emission values and quenching percentage at specific concentrations of metal.

In the analysis of Cd^{2+} effects on the AsGFP fluorescence intensity, a quenching about of 9% at 31 µM of cadmium was determined (fig. 46, table 9).

In figure 47 is shown the evolution of quenching of AsGFP fluorescence in presence of nickel (range of concentration from 0 to 96 µM) (table 10). Nickel influenced the fluorescence emission of GFP with a intensity decrement of 7% at 96 µM.

This quenching appeared insignificant rather the others metals tested.

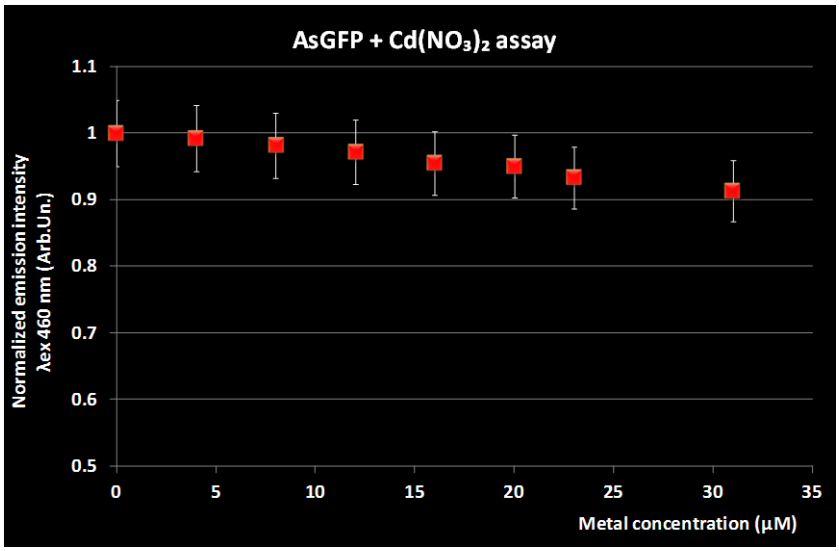

Fig. 46. Evolution of quenching of AsGFP by cadmium solution.

Cd^{2+} concentration (µM)	*Emission (Arb. Un.)*	*% Quenching*
0	1	0
4	0.992	0.8
8	0.982	1.8
12	0.972	2.8
16	0.955	4.5
20	0.950	5.0
23	0.933	6.7
31	0.914	8.6

Table 9. Range of cadmium concentrations used in the AsGFP assays. Normalized emission values and quenching percentage at specific concentrations of metal.

In figure 48 a summary of the evolution of AsGFP maximum intensity emission with copper, lead, nickel and cadmium is shown. The reactivity is different for every metal investigated and it is evident by the observation of the trend of fluorescence decline by all metals tested. The higher effect of quenching is determined by copper and lead while the quenching of cadmium and nickel is not much evident. At about 32 µM of metal

concentration a quenching of 35% for Cu^{2+}, 17% for Pb^{2+}, 9% for Cd^{2+} and 7% for Ni^{2+} is measured (fig. 49).

Irrelevant quenching effect was found for HNO_3 and NaCl.

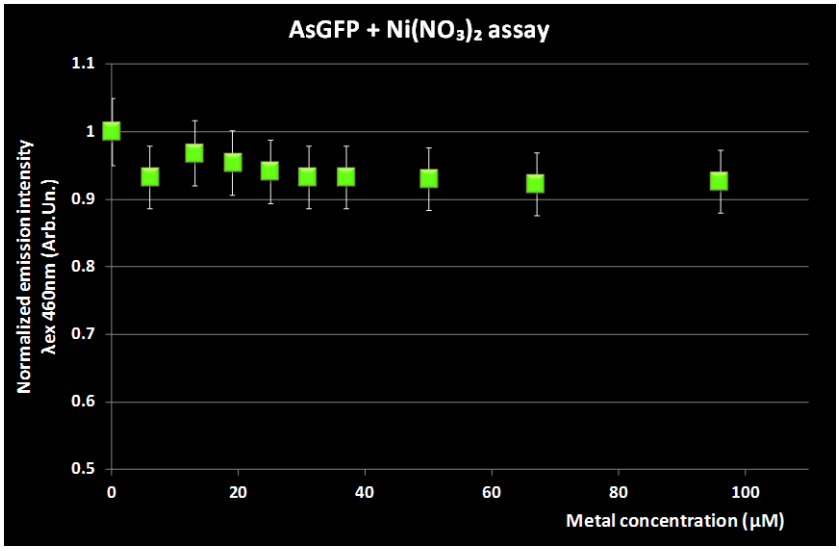

Fig. 47. Evolution of quenching of AsGFP by nickel solution.

Ni^{2+} concentration (µM)	*Emission (Arb. Un.)*	*% Quenching*
0	1	0
6	0.933	6.7
13	0.968	3.2
19	0.954	4.6
25	0.941	5.9
31	0.933	6.7
37	0.933	6.7
50	0.930	7
67	0.923	7.7
96	0.926	7.4

Table 10. Range of nickel concentrations used in the AsGFP assays. Normalized emission values and quenching percentage at specific concentrations of metal.

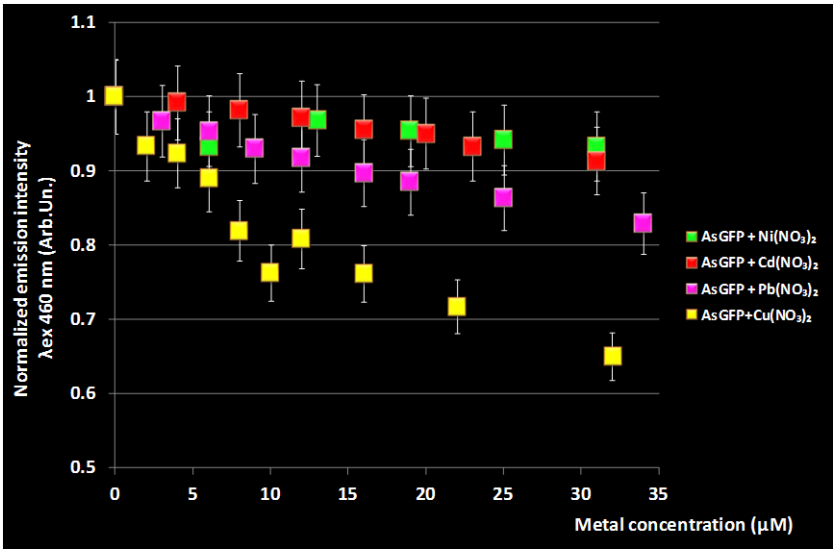

Fig. 48. Summary of AsGFP quenching evolution in presence of all metals solutions.

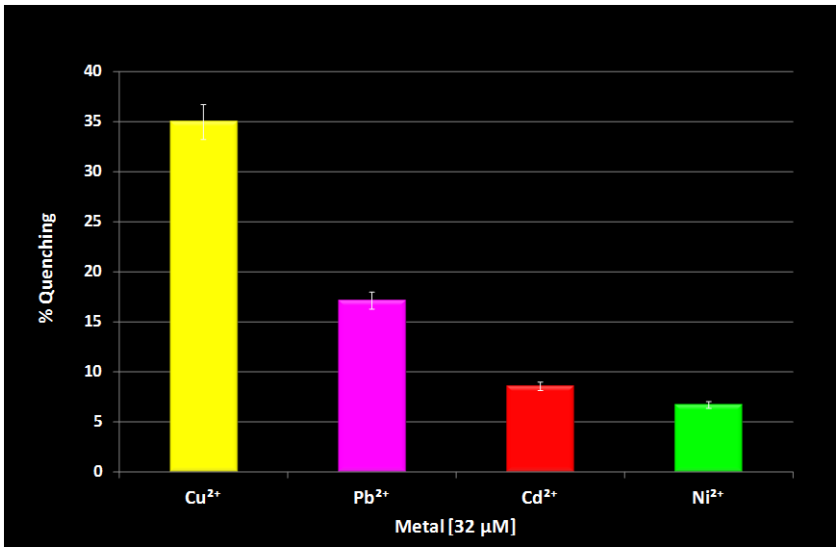

Fig. 49. Histogram of the AsGFP quenching (%) at ~ 32µM of metals.

Only for AsGFP with Cu^{2+} a particular phenomena in the emission spectrum with λ_{ex} at 300 nm was observed. An effect of enhanced with a peak at about 350 nm in emission was recorded (fig. 50) while did not observe differences in the absorption spectrum. The attribution of the tryptophan peak is confirmed by the excitation spectrum (λ_{em} 350 nm) of AsGFP in presence of Cu^{2+} [22µM] (fig. 51).

The evolution of the enhancing effect on the fluorescence emission intensity of AsGFP in presence of copper is shown in figure 52.

A negative correlation between the emissions with λ_{ex} 460nm and λ_{ex} 300nm of AsGFP with copper is shown in figure 53.

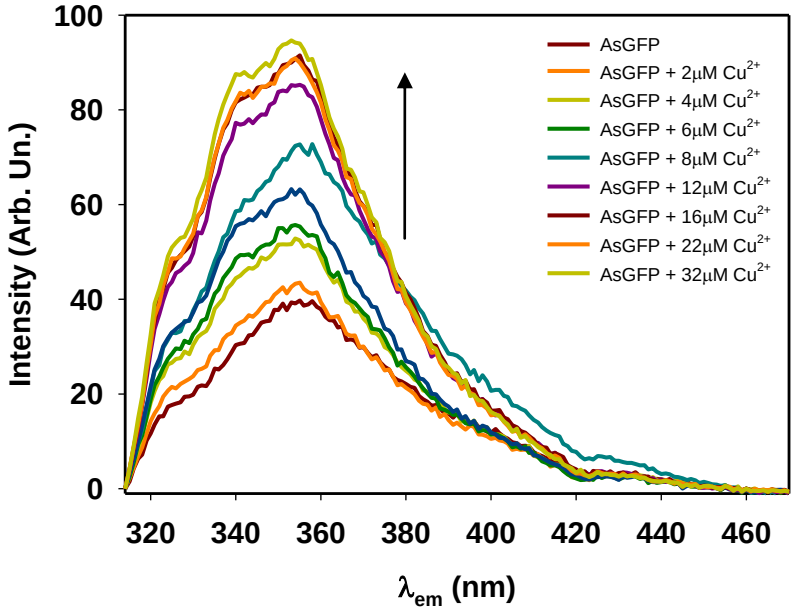

Fig. 50. Emission spectra of AsGFP with Cu^{2+} λ_{ex} 300nm. The arrow shows the enhancing of fluorescence intensity.

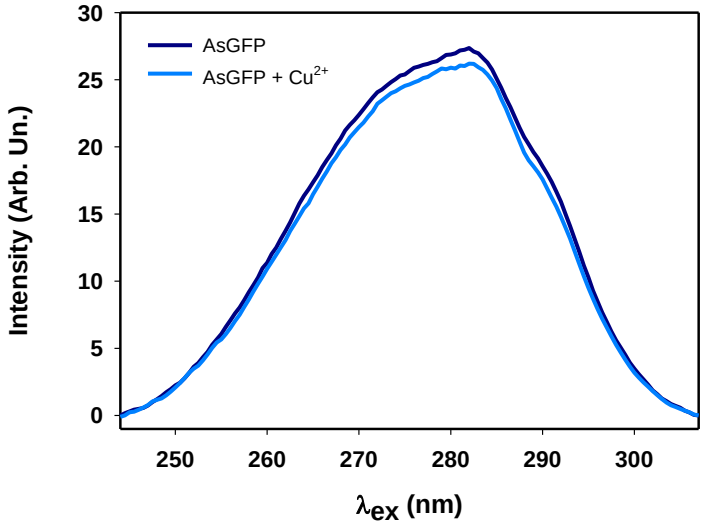

Fig. 51. Excitation spectra of AsGFP with Cu^{2+} [22 μM] λ_{em} 350nm. Range of excitation from 240 nm to 350 nm.

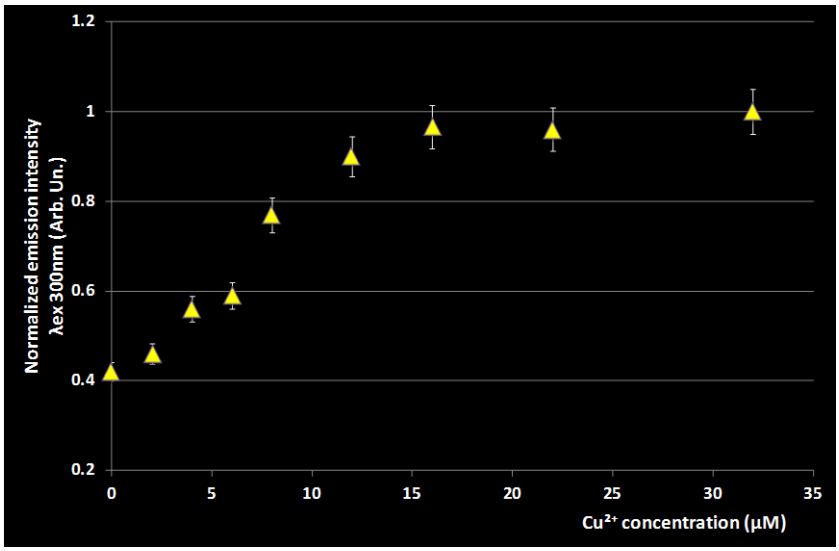

Fig. 52. Evolution of enhancing of AsGFP (λ_{ex} 300nm) by copper solution.

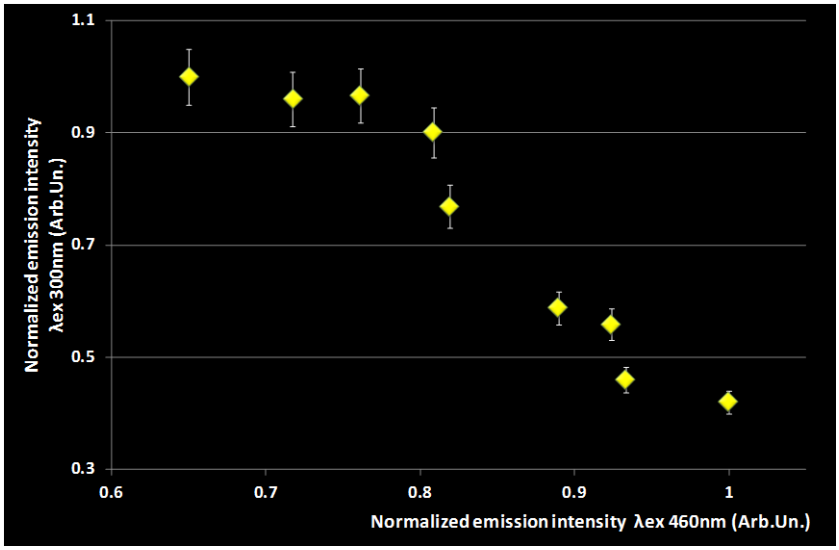

Fig. 53. Negative correlation of the emissions with λ_{ex} 460nm and with λ_{ex} 300nm of AsGFP with Cu^{2+}.

Then the metals assays on PPS, the attention was focused on AsGFP to value if a modification of the structure occurred. AsGFP control and treated (with copper) were

loaded on polyacrylamide gel in denaturing conditions. Results suggested that any modification on the AsGFP tetramer structure occurred in the treated sample (fig. 54).

Fig. 54. SDS-PAGE 10% in no reducing conditions. Line 1: PPS control (C); Line 2: PPS treated (T).

3.3.4. Dot Blot assay results

Fluorescence emission of partially purified sample is visualized in figure 55 A in which is evident as the different emission intensity is modified by the different concentration of protein (acquisition time 2 sec). This gel was imaged at the Versa-Doc Imaging System.

Then, according to the ChemiDoc for the bands quantization, the quenching effect of ~ 18% on the emission of PPS [100 nM] in presence of copper [40 µM] was determined (fig. 55 B).

This result is obtained considering that the maximum of intensity emission there is when protein is spotted without metal. The experiments were done in three replicates.

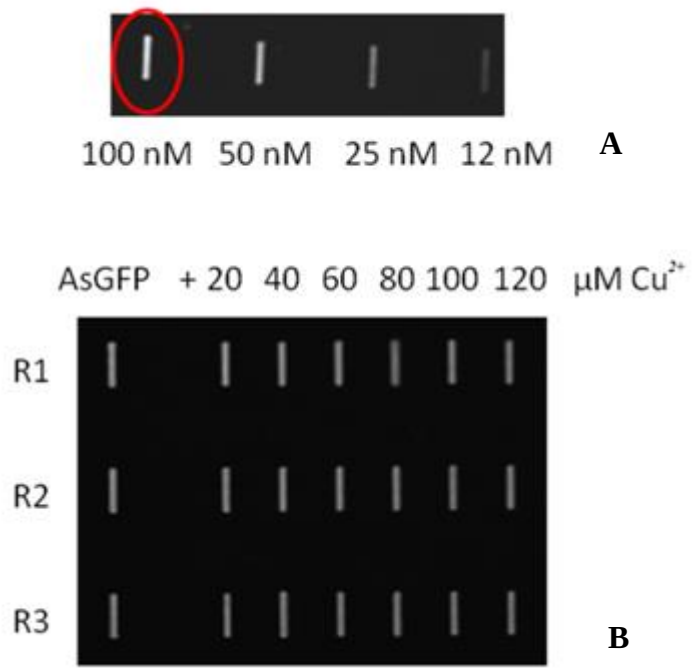

Fig. 55. A) Fluorescence emission of AsGFP on nitrocellulose membrane at different concentration. The red circle show the target protein concentration for the next assays. B) Assays of AsGFP with Cu^{2+} on nitrocellulose membrane. R1, R2 and R3 are the replicates.

3.4. Discussion

The SDS – PAGE of raw extract in no denaturing condition showed a single fluorescent band of ~ 124 KDa (fig. 33A). This result was indicative of a tetramer conformation of the protein (Wiedenmann *et al*., 2000) and that it was a non dissociable dimers (Ward, 1998). The denaturation with β-mercaptoethanol and the temperature (100°C) cracked the fluorescent band so it was not visible on gel after coloration with Comassie Brillian Blue (fig. 33B). These results are confirmed by results that Wiedenmann *et al*. (2000) obtained on asFP499/522 (table 2).

The eluted fractions obtained according to the gel filtration with Sephadex G 75 of raw extract, showed on SDS – PAGE a correct separation (fig. 35). In fact, this resin separated the proteins in function of molecular weight in the range from 3000 Da to 80000 Da. The protein pattern showed that the proteins eluted in the first time (min) had a band with a high molecular weight while in second time the resin eluted proteins with medium and lower molecular weight. Moreover, HPLC results confirmed the partially purification of 80%.

About the spectroscopic characterization of PPS, in the absorption spectrum many bands were obtained (fig. 36, 37).

The attribution of tryptophan peak was confirmed by the band obtained in the excitation spectrum (λ_{em} 350nm) of AsGFP with Cu^{2+} (fig. 51). In fact, the peak of emission at 350 nm was the peak of tryptophan (fig. 50).

In the emission spectrum of PPS (λ_{ex} 460 nm) many peaks were observed. At 500 nm and 519 nm (fig. 38, 40) there were the emission peaks of AsGFP, as Wiedenmann *et al*. (2000) reported.

The peaks in the red region of the spectrum were the characteristic peaks of chlorophyll *a* and carotenoids (Frigaard *et al*., 1996). In fact, the anemone has a symbiosis with unicellular dinoflagellates, the zooxantellae that allows anthozoans to thrive in oligotrophic waters (Leutenegger *et al*., 2007). The role of the single-cell algae which contains photosynthetic pigments in this symbiotic life is to produce oxygen and also photosynthesis products. On the other hand, these algae are protected by anemone from their predators. *A. sulcata* provides a hosting place to these alga and takes the products of these alga. Under normal conditions, this relationship is well protected; however,

some unwanted events such as pathogenic contamination and exposure to excessive UV radiation damage this relationship.

These data are confirmed by the results obtained according to the confocal spectroscopy on the tentacle of *Anemonia* in which two fluorescence species were discriminated (fig. 31, 32).

The experiments conducted on PPS showed as the emission intensity of protein was influenced by metals investigated.

The metal – protein bond seemed to be selective. Moreover, the bond effect changed with the different metals investigated (fig. 48). The order of quenching on the emission protein was Cu(II)>Pb(II)>Cd(II) (fig. 49). Moreover, this effect was more obvious at lower metal concentrations.

Quenching amplitudes were related to metal added. This evidence suggested:

- AsGFP behaviour depended from electronic orbitals of metals involved in bonds with the fluorophore neighbour;
- in the AsGFP structure both specific and unspecific bond sites would occurred.

Effects of Cu^{2+} and partially Pb^{2+} inducing larger changes in protein fluorescence, can be probably bonded to more specific donor groups that Cd^{2+} and Ni^{2+} whose additions induced only limited quenching effects.

These results suggested, a possible structural significance of recognized spectroscopic evidences. The copper ability to induce the quenching effect was determined by its dissolved phase. This suggested that the "metal – protein" bond occurred using the inner coordination sphere of copper. The recovery of fluorescence in presence of copper, using the EDTA suggested that the greatest steric size of the complex "metal – EDTA" probably did not allow the bond with the reactive protein group.

Copper is one of the two exceptions to the writing of electron configurations. One would expect copper to be an s^2d^9 ion. Instead, one electron is borrowed from the 4s orbital to completely fill the 3d orbital. Copper metal is therefore paramagnetic due to the unpaired electron in the orbital. The two most common ions formed by copper are the $^{+1}$ (cuprous) and $^{+2}$ (cupric). The cuprous ion is the less stable of the two oxidation states and is easily oxidized. Since electrons are lost first out of the 4s orbital, the electron configuration of the cuprous ion is $4s^03d^{10}$ and is therefore diamagnetic while the cupric ion is paramagnetic ($4s^03d^9$).

The paramagnetic characteristic of copper is assured by the enhancing effect observed in the emission spectrum (λ_{ex} 300nm) of AsGFP (fig. 50, 52). Probably Cu^{2+} with its unpaired electron in the *d* orbital determined some effect on the tryptophan. Near the fluorophore the trp90 is localized (fig. A, appendixes). The different effects observed in the investigated conditions (λ_{ex} 460nm/300nm) suggested a metal selectivity, in particular in the trp – Cu bond that was assured by the correlation between the enhancing effect at 350nm (tryptophan emission peak) and the quenching effect at 500/519nm (AsGFP emission peaks). Results allowed to think a possible conformational modification of protein when copper is added, in which the fluorophore or its residues, a tryptophan exposition was determined. The tetramer structure was unchanged (fig. 54).

Quenching results obtained for AsGFP with copper were comparable with results that Richmond *et al*. (2000) found in a mutants of GFP (high nanomolar concentration) from *A. victoria*, in which they introduced a site directed mutagenesis that conferred selective metal binding to GFP. They found a quenching of ~ 60% at 50µM of Cu^{2+}.

Different results were obtained by Isarankura *et al*. (2009) in a study on the spectroscopic behavior of copper ions using an His6GFP. A quenching of fluorescence of 60% was measured in the presence of 500 µM of copper and of 30% for 50µM of copper with a concentration of His6GFP at 0.5 µM . As with our experiments, the observed the recovery of original fluorescence through the addition of EDTA they observed.

Tansila *et al*. (2008) did not find any significant effects from Co^{2+} and Ni^{2+} in many variants of GFP from *A. victoria* with a superfolder mutation and additional mutagenesis for histidines. They found a 25% of quenching by copper in a mutant with the histidine situated closer to the fluorophore.

Sumner *et al*. (2006) found on DsRed a quenching effect of 90±10% and 75±10% at 2.5µM of Cu^{2+} and Cu^{+} respectively.

Copper ions prefer coordination with amines, ionized peptide nitrogens and thiolates (Silvia *and* Williams, 1991); structural motifs that have high affinity for Cu^{2+} are frequently composed of the side chains of His, Tyr, Glu, Asp, Cys, and sometimes Asn and Gln (Sigel *and* Martin, 1982).

In AsGFP, a histidine, His60, is found on the opposite side of the hydroxyphenyl group (Fig. A, appendixes), where its imidazole side chain is held in place in an almost

perpendicular orientation with respect to the phenyl ring by hydrogen bonds of its ring nitrogens to three water molecole (Nienhaus *et al*., 2006) (fig. 2C).

Only the fluorophores exposed on the protein surface can be dynamically quenched whereas when they are located in the internal structure of protein, they are quenched by static process. In the case of AsGFP, the chromophore is inside at β-barrel that does not allow the access at ligand. Rahimi *et al*. (2008) reported for DsRed, that "*Cu^{2+} forms a complex with specific amino acids on the protein. This complex formation can lead to formation of non-fluorescent species in three ways, i) by affecting hydrogen-bonding network of the chromophore, ii) by bringing Cu^{2+} close to chromophore such that it contacts the excited-state of the chromophore, iii) by causing conformation/structural changes in the protein*".

The quenching effect result by copper obtained on PPS, using the dot blot assay, was different rather the spectroscopic results. In the dot blot assay any control system was used (as the absorption measures in the spectroscopic assays) to value the protein denaturation or others phenomena that could determine quenching effect. So, this device was not useful to value the effect of metal on the fluorescence emission.

3.5. Conclusions

In this study, the spectroscopic properties of a wild type GFP from *A. sulcata* in presence of environmental contaminants were investigated.

Different results was obtained for AsGFP about the evolution and the value of quenching effect on the fluorescent emission for all metals investigated. In fact, the metal – protein bond seemed to be selective and the bond effect changed with the different metals investigated. The order of quenching on the emission protein was Cu(II)>Pb(II)>Cd(II).

The different effects observed in the investigated conditions (λ_{ex} 460nm/300nm) suggested a metal selectivity, in particular in the trp – Cu bond.

Results allowed to think a possible conformational modification of protein when copper is added, in which the fluorophore or its residues determined, a tryptophan exposition. The tetramer conformation was not changed.

The future study of the possible modification of cellular and sub cellular tentacle ectodermic portion in presence of metal ions, through in vivo assays on *A. sulcata* and the analysis of the fluorescence behavior of recombinant GFP in the same conditions could allow to think at the system as potential device sensor.

There is an enormous demand for optical sensors in many areas, such as the environmental monitoring, industrial and food processing, healthcare, biomedical technology, and clinical analysis, where high sensitivity and ease of operation are two main issues (Shi *et al*., 2004; Jeronimo *et al*., 2007). Fluorescence technique can easily fulfill both requirements and has been widely applied in the fields of chemical sensing and biosensing (Jiang *and* Guo, 2004; Prodi, 2005; Lim *and* Lippard, 2007). In the design of fluorescence-based sensors, the fluorescence probes remain a key determinant to the future success of the sensor. Therefore, the development of fluorescence probes has been a long-term and attractive topic among the scientists (Callan *et al*., 2005; Demchenko, 2005). In this regard, many kinds of fluorophores have been developed, and already been applied in the sensors design. Unfortunately, the performance of these established fluorescent sensors are greatly limited by using the conventional fluorescence probes. For instance, organic fluorophores, which are most commonly used in fluorescence technique, suffer from low brightness and poor photostability, which lead to reduced sensitivity and stability of the sensor (Zhou *and* Zhou, 2004; Demchenko, 2005; Prodi, 2005). In addition, organic fluorophores tend to have small Stokes shifts, thus limiting their utility in the fields, such as ratiometric measurements and fluorescence resonance energy transfer (FRET)- based detection (Demchenko, 2005). Compared with conventional organic fluorophores, the recently developed semiconductor quantum dots show great promise as the fluorescence probes due to their improved photophysical properties, including high quantum yield, size-tunable narrow emissions and minimal photobleaching (Costa-Fernaˇındez *et al*., 2006; Somers *et al*., 2007). However, these nanocrystalline materials still suffer from several issues, such as the harsh and toxic conditions in the synthesis, large physical size, strong non-molecular low-power fluorescence intermittency, which also limit their further application in fluorescence sensing research (Verberk *et al*., 2002; Derfus *et al*., 2004; Vosch *et al*., 2007). Therefore, the development of new fluorophores that can challenge the above problems is of great importance for both fluorescence sensing and other fluorescence-based applications like fluorescence imaging (Rao *et al*., 2007).

Specimen	FP	Color	Absorption/excitation maxima (nm)	Emission maxima (nm)	MW (kDa)	Reference
A. sulcata var. rufescens	asFP499/522	verde	< 280/400/480/511	499/522	26.2[a] / 23.0[b] / 66.0[c]	Wiedenmann *et al* ., 2000
A. sulcata var. rufescens	asFP595	arancio	278/337/ 574	595	19.1[a] / 66.0[bc]	Wiedenmann *et al* ., 2000
A. sulcata var. rufescens	asCP562	red	562	595§	19.1[a] / 66.0[bc]	Wiedenmann *et al* ., 2001
A. sulcata var. smaragdina	asFP499	verde	< 280/400/480/511	499/522	25.4[a]	Leutenegger *et al* ., 2007

Table 1. Spectroscopic and biochemical characteristics of different morph of *A. sulcata*. *by SDS-PAGE. † by gel filtration in denaturing conditions. ‡by gel filtration in physiological conditions. §Then a denaturation-renaturation process. (Wiedenmann *et al.*, 2000).

Treatment	65°C/5 min	80°C/5 min	95°C/2.5 min	1% SDS	8 M Urea	pH 5.5	pH 11	200 mM β-Mer-captoethanol	Mineral oil	4% Paraformaldehyde
asFP499/522*	+++++	+	+	+++ (502 nm)†	+++++	+++	++ (509 nm)†	+++++	++++	(d.)
asFP595*	+++++	++++	++	++	++++ (600 nm)†	+++	+	+++++	+++++	(d.)
asCP562	(d.)	(d.)	(d.)	(d.)	(d.)	(d.)	(n.d.)	(d.)	(d.)	(d.)

Table 2. Stability of pigments isolated from *A. sulcata.* (Wiedenmann *et al.*, 2000).
(d.), detectable; (n.d.), not detectable. *+++++ = >90%; ++++ = 75–79%; +++ = 30–35%; ++ = 15–20%; + = <10%. †Shifts of emission (Wiedenmann *et al.*, 2000).

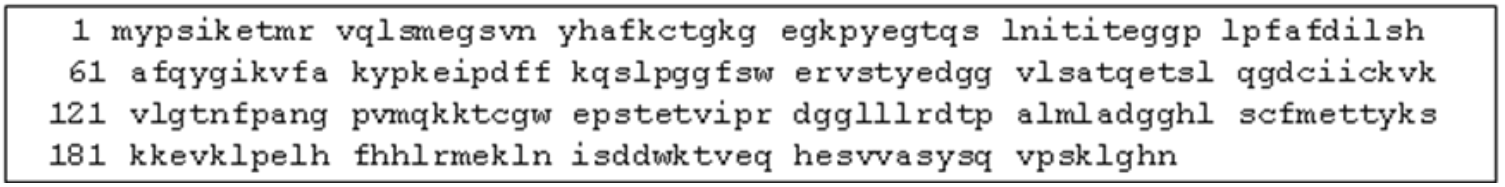

Fig. A. Aminoacid sequence of AsFP499 (Genbank AAG41205.1).

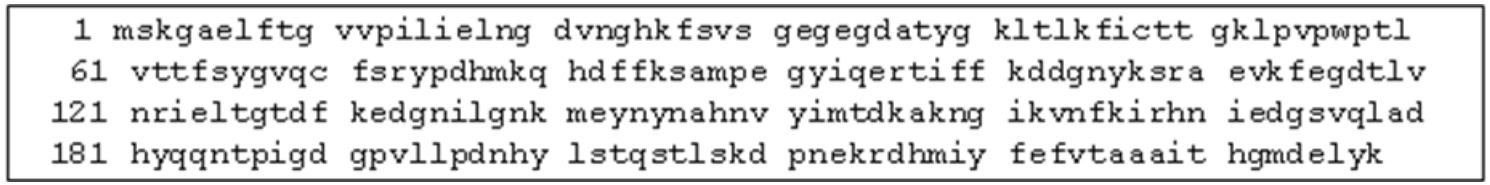

Fig. B. Aminoacid sequence of rAcGFP (Genbank AAN41637.1).

Acknowledgments

I would like to start by expressing my very sincere thanks to Angela Cuttitta e Salvatore Mazzola who believed in me in these three years of hard work and made it possible by accepting me in their research group. Thanks to them my passion for the scientific research, the constancy and my self confidence increased.

Warm thanks to Paolo Censi for his willingness to meet my needs, uncertainties, fears and for allowing the realization of this work.

A special thanks to Valeria Vetri for her continuous and essential assistance.

Many thanks also to Monica Salamone, Prof. Ghersi, Prof. Militello, Paolo Colombo and Filippo Saiano for hosting me in their laboratories and putting me at ease.

The assistance of Anna Lisa Alessi for reviewing the English text is acknowledged.

Last but not least, I would like to thank Luca and my little son, Marco, for grinning and bearing my frequent absences without feeling me guilty about it.

Many thanks also to my family and few but special friends for their continuous practical and moral support.

References

Agmon N., 2005. Proton pathways in green fluorescent protein. *Biophys. J.* **88**: 2452–2461.

Ando R., Mizuno H., Miyawaki A., 2004. *Science* **306,** 1370–1373.

Andresen M., Wahl M.C., Stiel A.C., Grater F., Schafer L.V., Trowitzsch S., Weber G., Eggeling C., Grubmuller H., Hell S.W., Jakobs S., 2005. *Proc. Natl. Acad. Sci. USA* **102**, 13070.

Baird G.S., Zacharias D.A., Tsien R.Y., 2000. *Proc. Natl Acad. Sci. USA*. **97**: 11984-11989.

BD Living Colors AcGFP1 Fluorescent Protein, 2005. *Clontechniques*.

Bozkurt S.S., Cavas L., 2008. Can Hg(II) be Determined via Quenching of the Emission of Green Fluorescent Protein from *Anemonia sulcata* var. *smaragdina*? *Applaied Biochemistry and Biotechnology*.

Brandt J.F., 1838. Ausführliche beschreibung der von C.H. Mertens auf seiner Weltumsgelung beobachten Schirmuallen nebst allgemeine Bemerkungen über die Schirmuallen überhaupt. Mém. Acad. Imp. Sci. St. Pétersbourg, Sér. **6**, 4(2):237-411.

Callan J.F., De Silvaa A.P., Magri D.C., 2005. *Tetrahedron* **61**, 8551–8588.

Catala, R., 1959. *Nature (London)* **183**, 949.

Chakraborty P., Babu P.G., Alam A., Chaudhari A., 2008. GFP expressing bacterial biosensor to measure lead contamination in aquatic environment. *Current Science*, **94**(6): 800-805

Chalfie, M., 1995. Green fluorescent protein. *Photochem. Photobiol*. **62**, 651–656

Chapleau R.R., Blomberg R., Ford P.C., Sangermann M., 2008. Design of a highly specific and noninvasive biosensor suitable for real-time in vivo imaging of mercury (II) uptake. *Protein Science*, **17**:614–622.

Chudakov, D. M., Belousov, V. V., Zaraisky, A. G., Novoselov, V. V., Staroverov, D. B., Zorov, D. B., Lukyanov, S. & Lukyanov, K. A., 2003. *Nat. Biotechnol.* **21,** 191–194. Doubilet, P., 1997. *Nat. Geogr.* **192**, 32–43.

Costa-Fernaˇındez J.M., Pereiro R., Sanz-Medel A., 2006. *Trends Anal. Chem*. **25**, 207–218.

Demchenko A.P., 2005. *Anal. Biochem*. **343**, 1–22.

Derfus A.M., Chan W.C.W., Bhatia S.N., 2004. *Nano lett*. **4**, 11–18.

Dove S.G., Hoegh-Guldberg O., Ranganathan S., 2001. Major colour patterns of reefbuilding corals are due to a family of GFP-like proteins. *Coral Reefs*.**19**: 197-204.

Eli P., Chakrabartty A., 2006. Variants of DsRed fluorescent protein: Development of a coppere sensor. *Protein Science*, **15**: 2442-2447.

Fradkov, A.F., Verkhusha, V.V., Staroverov, D.B., Bulina, M.E., Yanushevich, Y.G., Martynov, V.I., Lukyanov, S., Lukyanov, K.A., 2002. Far-red fluorescent tag for protein labelling. *Biochem. J*. 368, 17–21.

Frigaard N.U., Larsen K., Cox R.P., 1996. Spectrochromatography of photosynthetic pigments as a fingerprinting technique for microbial photrops. *FEMS Microbiology Ecology* **20**: 69-77.

Fu Y., Zhang J., Lakowicz J.R., 2008. Metal-enhanced fluorescence of single green fluorescent protein (GFP). *Biochemical and Biophysical Research Communications*, **376**: 712–717.

Gurskaya N.G., Fradkov A.F., Pounkova N.I., Staroverov D.B., Bulina M.E., Yanushevich Y.G., Labas Y.A., Lukyanov S., Lukyanov K.A., 2003. *Biochemical Journal*, **373**, 403-408.

Helms V., 2002. *Curr. Opin. Struct. Biol.*, **12**, 169.

Hsiu-Chuan Liao V., Chien M.T., Tseng Y.Y., Ou K.L., 2006. Assessment of heavy metal bioavailability in contaminated sediments and soils using green fluorescent protein-based bacterial biosensors. *Environmental Pollution*, **142**:17-23.

Isarankura-Na-Ayudhya C., Suwanwong Y., Boonpangrak S., Kiatfuengfoo R., Prachayasittikul V., 2005. Co-expression of zinc binding motif and GFP as a cellular indicator of metal ions mobility. *Int. J. Biol. Sci.*, **1**: 146-151.

Isarankura-Na-Ayudhya C., Tantimongcolwat T., Galla H.J., Prachayasittikul V. 2009. Fluorescent Protein-Based Optical Biosensor for Copper Ion Quantitation. *Biol Trace Elem Res*.

Jeronimo P.C.A., Araujo A.N., Conceicao M., Montenegro B.S.M., 2007. *Talanta* **72**,13–27.

Jiang P., Guo Z., 2004. *Coord. Chem. Rev*. **248**, 205–229.

Johnson, F. H., Shimomura, O., Saiga, Y., Gershman, L. C., Reynolds, G. T., and Waters, J. R., 1962. *J. Cell. Comp. Physiol.* **60**, 85-104

Kawaguti S., 1944. On the physiology of reef corals VI. Study on the pigments. *Palao Trop. Biol. Stn. Stud*. **2**: 617-674.

Kawaguti, S., 1966. *Biol. J. Okayama Univ.* **2**, 11–21.

Lauf U., Lopez P., Falk M.M., 2001. *FEBS Lett.* **498**: 11-15.

Leiderman P.,, D. Huppert, N. Agmon, 2006. *Biophys. J*. **90**, 1009.

Leutenegger A., Kredel S., Gundel S., D'Angelo C., Salih A., Wiedenmann J., 2007. Analysis of fluorescent and non-fluorescent sea anemones from the Mediterranean Sea during a bleaching event. *Journal of Exparimental Marine Biology and Ecology*, **353**:221-234.

Lim M.H., Lippard S.J., 2007. *Acc. Chem. Res*. **40**, 41–51.

Lukyanov, K. A., Fradkov, A. F., Gurskaya, N. G., Matz, M. V., Labas, Y. A., Savitsky, A. P., Markelov, M. L., Zaraisky, A. G., Zhao, X. N., Fang, Y., 2000. *J. Biol. Chem.* **275,** 25879–25882.

Matz M.V., Fradkov A.F., Labas Y.A., Savitsky A.P., Zaraisky A.G., Markelov M.L., Lukyanov S.A., 1999. *Nat. Biotechnol.*, **17**:969-973.

Mazel, C. H., 1995. *Mar. Ecol. Prog. Ser*. **120**, 185–191.

Mazel, C. H., 1997. *Ocean Optics XIII SPIE* **2963**, 240–245.

Mizuno H., Sawano A., Eli P., Hama H., Miyawaki A., 2001. *Biochemistry*. **40**: 2502-2510.

Mizuno T., Murao K., Tanabe Y., Oda M., Tanaka T., 2007. Metal-ion-dependent GFP Emission in Vivo by Combining a Circularly Permutated Green Fluorescent Protein with an Engineered Metal-Ion-Binding Coiled-coil. *J. Am. Chem. Soc.*, **129** (37):11378-11383.

Morise H., Shimomura, O. et al.,1974. *Biochemistry* **13:** 2656-2654.

Nienhaus K., Renzi F., Vallone B., Wiedenmann J., Nienhaus G.U., 2006. Chromophore-Protein Interactions in the Anthozoan Green fluorescent Protein asFP499. *Biophysical Journal*, **91**: 4210-4220.

Ormo M., Cubitt, A. B., Kallio, K., Gross, L. A., Tsien, R. Y. & Remington, S. J., 1996. *Science* **273**, 1392–1395.

Peres J.M., 1982. General features of organismic assemblages in pelagial and benthal. In: O.Kinne (ed.) *Marine Ecology*, vol 5, Ocean management Part 1, Wiley, Chichester, 9-581.

Prodi L., 2005. *New J. Chem*. **29**, 20–31.

Quillin M.L., Anstrom D. A., Shu X. K., ORLeary S., Kallio K., Chudakov D. A., Remington S. J., 2005. *Biochemistry*, **44**, 5774.

Rahimi Y., Goulding A., Shrestha S., Mirpuri S., Deo S.K., 2008. Mechanism of Copper Induced Fluorescence Quenching of red Fluorescent Protein, DsRed. *Biochem Biophys Res Commun*., **370**(1):57-61.

Rao J., Dragulescu-Andrasi A., Yao H., 2007. *Curr. Opin. Biotechnol*. **18**, 17–25.

Richmond T., Takahashi T.T., Shimkhada R., Bernsdorf J., 2000. Engineered Metal Binding Sites on Green Fluorescent Protein. *Biochemical and Biophysical Research Communications.* **268**: 462-465.

Roberto R.R., Barnes J.M., Bruhn D.F. 2002. Evaluation of a GFP reporter gene construct for environmental arsenic detection. *Talanta.* **58:** 181–188

Schafer L.V., Groenhof G., Grubmuller H., Klingen A., Ullmann G.M., Pasqua M.B., Robb M.A., 2007. Photoswitching of the fluorescent protein asFP595: mechanism, Proton Pathways, and Absorption Spectra. *Angew. Chem*. 2007, **119**, 536 –542

Schlichter, D., Fricke, H. W. & Weber, W., 1986. *Mar. Biol.* **91**, 403–407.

Schlichter, D., Fricke, H. W. & Weber, W., 1988. *Endocyt. C. Res.* **5,** 83–94.

Shagin D.A., Barsova E.V., Yanushevich Y.G., Fradkov A.F., Lukyanov K.A., Labas Y.A., Semenova T.N., Ugalde J.A., Meyers A., Nunez J.M., Widder E.A., Lukyanov S.A., Matz M.V**.,** 2004. GFP-like Proteins as ubiquitous Metazoan superfamily: Evolution of functional features and structural complexity. *Mol. Biol. Evol*. **21**: 841-850.

Shi J., Zhu Y., Zhang X., Baeyens W.R.G., Garcia-Campana A.M., 2004. *Trends Anal.Chem*. **23**, 351–360.

Shimomura, O., 1979. *FEBS Letters* **104:** 220-222.

Sigel, H. and Editor, 1982. Metal Ions in Biological Systems, **12**: Properties of Copper.

Silvia, J., Williams, R., 1991. The Biological Chemistry of the Elements: The Inorganic Chemistry of Life. *Claredon Press*, Oxford.

Sniegowski, J. A., Lappe J. W., Patel H. N., Huffman H. A., Wachter R. M., 2005. Base catalysis of chromophore formation in Arg96 and Glu222 variants of green fluorescent protein. *J. Biol. Chem*. **280**: 26248–26255.

Somers R.C., Bawendi M.G., Nocera D.G., 2007. *Chem. Soc. Rev*. **36**, 579–591.

Stoner-Ma D., Jaye A. A., Matousek P., Towrie M., Meech S. R., Tonge P. J., 2005. *J. Am. Chem. Soc.*, **127**, 2864.

Sumner J.P., Westerberg N.M., Stoddard A.K., Hurst T.K., Cramer M., Thompson R.B., Fierke C.A., Kopelman R., 2006. DsRed as a highly sensitive, selective, and reversible

fluorescence-based biosensor for both Cu+ and Cu2+ ions. *Biosensors and Bioelectronics*, **21**:1302–1308.

Surpin, M. A. & Ward, W. W., 1989. *Photochem. Photobiol.* **49,** 65.

Tansila N., Becker K., Isarankura Na-Ayudhya C., Prachayasittikul V., Bulow L., 2008. Metal ion accessibility of histidine-modified superfolder green fluorescent protein expressed in Escherichia coli. *Biotechnol lett*. **30**:1391-1396.

Tasdemir A., Khan F., Jowitt T.A., Iuzzolini L., Lohmer S., Corazza S., Schmidt T.J., 2008. Engineering of a monomeric fluorescent protein AsGFP499 and its applications in a dual translocation and transcription assay. *Protein Engineering, Design & Selection*. 1-10.

Taylor C.J., Bain,L.A., Richardson D.J.,Spiro S., Russell D.A., 2004. Construction of a whole-cell gene reporter for the fluorescent bioassay of nitrate. *Analytical Biochemistry*, **328**:60–66.

Trautwein, A.X. (Ed.), 1997. Bioinorganic Chemistry. *Wiley-VCH*, Weinheim.

Tsien, R., 1998. *Annu. Rev. Biochem.* **67**: 509-544.

Vendrell O., Gelabert R., Moreno M., Lluch J. M., 2006. *J. Am. Chem. Soc*., **128**, 3564.

Verberk R., Van Oijen A.M., Orrit M., 2002. *Phys. Rev.* B **66**, 233202.

Vosch T., Antoku Y., Hsiang J., Richards C.I., Gonzalez J.I., Dickson R.M., 2007. *Proc.Natl. Acad. Sci.* **104**, 12616–12621.

Voityuk A. A., Michel-Beyerle M. E. & Ro¨sch N., 1998. *Chem.Phys.* **231,** 13.

Wall M. A., Socolich, M. & Ranganathan, R., 2000. *Nat. Struct. Biol.* **7,** 1133–1138.

Ward W. W., 1998. In *Green Fluorescent Protein: Properties, Applications, and Protocols*, eds. Chalfie, M. & Kain, S. (Wiley, New York), pp. 45–75.

Wiedenmann J., Elke C., Spindler K.D., Funke W., 2000. Cracks in the b-can: Fluorescent protein from Anemonia sulcata. *Proc. Natl Acad. Sci.USA*. 97 (26) 14091-14096.

Wiedenmann J., Schenk A., Rocker C., Girod A., Spindler K.D., Nienhaus G.U., 2002 – A Far-red fluorescent protein with fast maturation and reduced oligomerization tendency from *Entacmaea quadricolor* (Anthozoa, Actinaria). *PNAS*, **99**(18): 11646-11651.

Wiedenmann, J., 1997. Offenlegungsschrift DE 197 18 640 A1 (Deutsches Patent-und Markenamt), pp. 1–18.

Wilmann P.G., Petersen J., Devenish R. J., Prescott M., Rossjohn J., 2005. *J. Biol. Chem.*, **280**, 2401.

Wood, T. I., Barondeau D. P., Hitomi C., Kassmann C. J., Tainer J. A., Getzoff E. D., 2005. Defining the role of arginine 96 in green fluorescent protein fluorophore biosynthesis. *Biochemistry*. **44**:16211– 16220.

Yang F., Moss L.G., Phillips G.N., 1996 - The molecular structure of green fluorescent protein. *Nat. Biotechnol*. **14**:1246–1251.

Yang T.T., Cheng L., Kain S.R., 1996b – *Nucleic Acids Res*. **24**: 4592-4593.
Yarbrough, D., Wachter, R. M., Kallio, K., Matz, M. V. & Remington, S. J. 2001. *Proc. Natl. Acad. Sci. USA.* **98,** 462–467.

Zhou X., Zhou J., 2004. *Anal. Chem*. **76**, 5302–5312.